Preparation and Applications of

Polyvinyl Alcohol-funtionalized Multiwalled Carbon Nanotubes for

Proton Exchange Membrane Fuel Cells

A Major Qualifying Project Report

Submitted to the Faculty of

Chemical Engineering Department

WORCESTER POLYTECHNIC INSTITUTE

in partial fulfillment of the requirements for

Degree of Bachelor of Science

By

_____

Hang Nguyen

Date: 01/15/2011

Approved by

_____ _____

Professor Ying-Ling Liu, Advisor **Professor Yi Hua Ma, Co-advisor**

ACKNOWLEDGEMENTS

First of all, I would like to thank Professor Liu and Professor Ma for giving me the opportunity to work on this project. I am very grateful that Professor Liu kindly provided me the research topic and guidance for my work as well as the access to his lab at Chemical Engineering Department and at R&D Center for Membrane Technology in Chung Yuan Christian University (CYCU), Chung Li, Taiwan. A special thanks to Professor Ma who became my advisor at WPI as he helped me with the application for going abroad to Taiwan and helped me to prepare for the research prior to doing lab-work in Taiwan. I would also like to thank the management team at Chung Yuan Christian University and Membrane Center for granting me the privilege of using all the necessary facility for my work and thanks to their generosity of providing me with housing during my stay in Taiwan. Last but not least, thanks to Chia-Ming Chang, Chia Chia, and Chia Yun who are graduate students at CYCU for being there instructed me with operating machinery, showed me how to do things, answered my questions, and discussed with me about lab results.

ABSTRACT

Modification of Nafion membranes using multiwalled carbon nanotubes (MWCNTs) was investigated in recent research for the enhancement of proton exchange membrane fuel cell performances. Incorporating polymers such as polyvinyl alcohol into MWCNTs suggested an improved compatibility between modified CNTs and Nafion matrix. In this project, polyvinyl alcohol (PVA) was chemically bonded to multi-walled carbon nanotubes (MWCNTs) by ozone mediated process. The PVA-functionalized carbon nanotube (CNT-PVA) was characterized using Attenuated total reflection - Fourier transform infrared spectroscopy, Thermogravimetric analysis, X-ray photoelectron spectroscopy, and solubility test. Three different kinds of CNT-PVA modified Nafion membranes were prepared: recast Nafion which included 0 wt% of CNT-PVA, CNT-PVA/Nafion 0.05 which included 0.05 wt% of CNT-PVA, and CNT-PVA/Nafion 0.1 which included 0.1 wt% of CNT-PVA. All of the above mentioned Nafion membranes, together with commercial Nafion, were tested in mechanical strength using Instron analysis. Conductivity tests were conducted to compare the conductive performances of commercial Nafion-212, recast Nafion, CNT-PVA/Nafion 0.05 and CNT-PVA/Nafion 0.1. Two composite membranes were proved to possess better mechanical properties than commercial Nafion 212 and recast Nafion membrane; nevertheless, commercial membrane demonstrated greater proton conductivity than those of modified membranes.

Table of Contents

Table of Figures

Table of Tables

Chapter 1. INTRODUCTION

1.1. Fuel Cell Developments

Fuel cells have received extensive recognition as an alternative renewable method of energy generation. Fuel cells are devices that convert chemical energy into electrical energy using two reactants, a fuel and an oxidant, and an electrolyte. As opposed to traditional batteries, which chemically store a limited amount of electrical energy, fuel cells can operate continuously with the replenished external flows of reactants. Fuel cell technology offers many advantages such as pollution free – no gaseous pollutants like CO or NO_x, high efficiency, and simple structure. Mechanically, fuel cells have no moving parts, thus having high durability, long lifetime, and silent performance. Unlike internal combustion engines using gasoline or diesel, fuel cells are not subject to the second law of thermodynamics or the Carnot maximum cycle efficiency, due to its ability to bypass irreversible thermal steps during the electrochemical conversion process.

It was reported that Welsh scientist William Grove invented the first fuel cell in 1839 (Hoogers, 2003.) In the early 1960s, Thomas Grubb and Leonard Niedrach working for General Electric Company (GE) successfully modified the original fuel cell design. Throughout the 1970s, GE continued developing proton exchange membrane (PEM) technology with NASA, U.S. Navy, and McDonnell Aircraft, leading to Project Gemini and Oxygen Generating Plant. Other groups, such as Los Alamos National Lab and Texas A&M University, also started looking into PEM fuel cells opportunities in the late 1980s and early 1990s (Smithsonian Institution, 2004). Recently, United Technology Corporation (UTC) has dominated the manufacture and commercialization of the fuel cell market, went on to making fuel cells for

automobiles, buses, cell phone towers and became the sole supplier to NASA Apollo missions as well as Space Shuttle Program.

Scientists have developed many different kinds of fuel cells, including alkaline fuel cells, molten carbonate fuel cells, phosphoric acid fuel cells, solid oxide fuel cells, metal hydride fuel cells, direct methanol fuel cells, and proton exchange membrane fuel cells. Each type of fuel cell has its own advantages and drawbacks, yet none is inexpensive and efficient enough to replace conventional ways of power generation.

1.2. Proton Exchange Membrane Fuel Cells (PEMFCs)

1.2.1. Components of PEMFCs

As shown in Figure 1, the PEMFC consists of two bipolar plates, two electrodes made up of catalysts in contact with Gas Diffusion Layers (GDLs) and a proton exchange membrane. The plates, usually made of metal or graphite, are placed on the outside of the cell through which the fuel (hydrogen) and the oxidant (oxygen) flow. The electrodes – anode and cathode, and the membrane together form the Membrane Electrode Assembly (MEA) which is the core of the PEMFC. GDLs are highly porous layers possessing significant electron conductive characteristic, typically made of carbon cloth or carbon fibers to enhance the diffusion rate (Gleason et al., 2008). Platinum or platinum alloys are often employed as catalysts to speed up the kinetics of the electrochemical reactions.

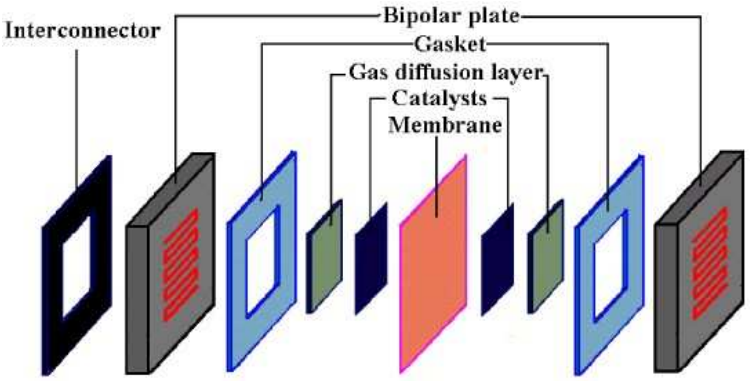

Figure 1. An exploded view of PEMFC components (Energi DTU Kemi, 2010).

1.2.2. How PEMFCs work

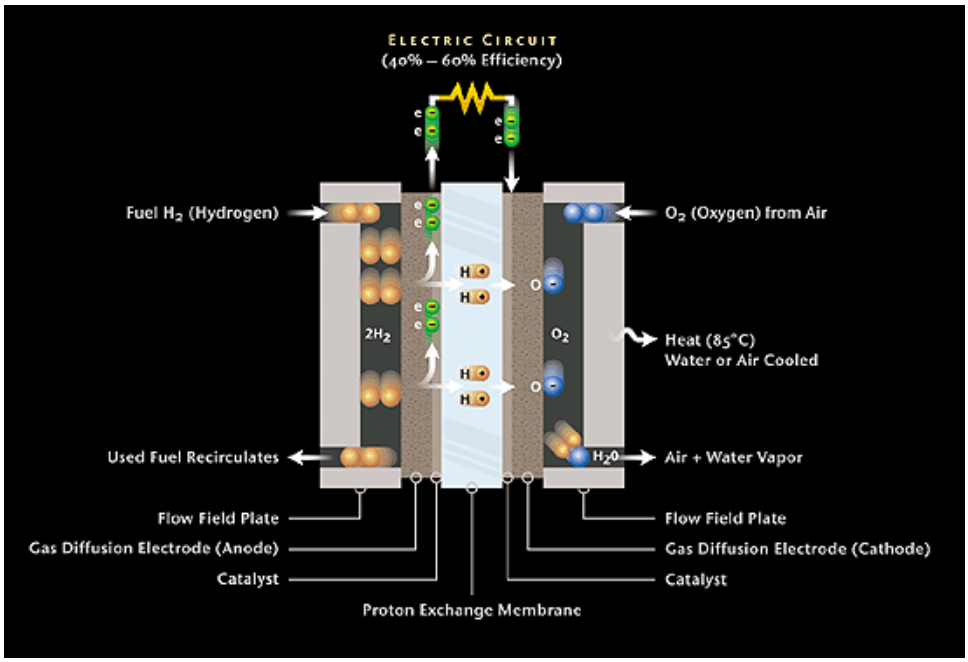

Figure 2. Schematic of Proton Exchange Membrane fuel cell (Fuel Cells Working Concept, 2006).

Anode: $H_2 \rightarrow 2H^+ + 2e^-$

Cathode: $\frac{1}{2} O_2 + 2H^+ + 2e^- \rightarrow 2 H_2O$

Overall: $H_2 + \frac{1}{2} O_2 \rightarrow H_2O$

Hydrogen atoms enter the cell at the anode side, travelling through the GDLs to reach reactive catalytic sites, where the first half-cell reaction happens; hydrogen is oxidized, forming ionized hydrogen atoms carrying positive charges called protons and free electrons. While the negatively charged electrons cannot pass through the polymer electrolyte membrane, all of the protons are allowed to permeate through the membrane to the cathode side. Current output of the cell is produced when the electrons travel along an external load circuit generated by the bipolar plates acting as current collectors. In the mean time, oxygen extracted from air is delivered to MEA cathode. Oxygen stream is then combined with the electrons returning from the electrical circuit and the protons arriving via the PEM to form water molecules. Used fuel hydrogen can be recycled and excess air and water vapor can also be collected.

The electrolytic membrane plays a key role in the inner-workings of the PEMFC. It is of importance for PEMFC function that the membrane only conducts appropriate ions between the anode and the cathode. Permitting other substances through can cause disruption of the chemical reactions: if free electrons are admitted, an effect known as “short circuit” would be created; if either gas can get to the other side of the cell, “gas crossover” problem would appear.

1.2.3. Limitations of PEMFCs

The performance of PEMFCs, measured in voltage at a certain current or power density, mainly depends on the proton conductivity of its membrane. Therefore, an increase by an order of magnitude in proton conductivity of the membrane would change the cell performance dramatically (Pillai et al., 2008). The conductivities of Nafion-based membranes, the most

widely used in PEM fuel cells, can be decreased by a number of reasons, including relative humidity and temperature of their operating environments. At temperatures above 80°C, Nafion starts exhibiting its inability to efficiently transport protons, thus leading to reduced cell performance (Pillai et al., 2010). The decline in thermal properties – chemical stability and mechanical strength - of Nafion at high temperature also need to be considered.

Working at higher temperature at approximately 150°C, however, is critical to prevent CO poisoning of Platinum catalyst besides the benefits of improved kinetics (Pillai, 2010). An option for eliminating problems associated with CO poison is to limit impurities present in hydrogen feed. Meanwhile, Carbon-supported Platinum catalysts have difficulties in splitting oxygen atoms at the cathode, driving electrical losses in PEMFCs (Smithsonian Institution, 2004). Consequently, catalytic activities can be improved by replacing Pt with a better material.

Moreover, the amount of water supplied and circulated inside the cell significantly affects cell power output. Too much water could flood the membrane while too little of it would dry the electrolytes (Field, 2008). Although the distribution of water is essential to cell performance, water has the tendency of being attracted toward the cathode due to polarization. Therefore, optimal water management poses an issue as well.

1.3. Nafion Membranes

Nafion®, industrial standard material for PEMFC membranes, is a supreme proton conductor developed and manufactured by DuPont. Nafion® dispersion D2020 has a polymer content of 20 wt% along with the mixture of water (34 ± 2 wt%), isopropanol (46 ± 2 wt%) and ethanol (< 2 wt%) as solvent.

Nafion membrane consists of a polytetrafluoroethylene (Teflon) backbone with hydrophilic side chains ending in sulfonic acid functional groups, which form clusters with water (Pillai et al., 2008). The sulfonic acid is an exceptional ion-conducting moiety due to the resonance stabilization of its conjugate base. If R-SO_3H loses H^+, the resulting negative charge is evenly relocated over three remaining oxygen atoms (Gleason et al., 2008). Figure 3 shows the molecular structure of Nafion.

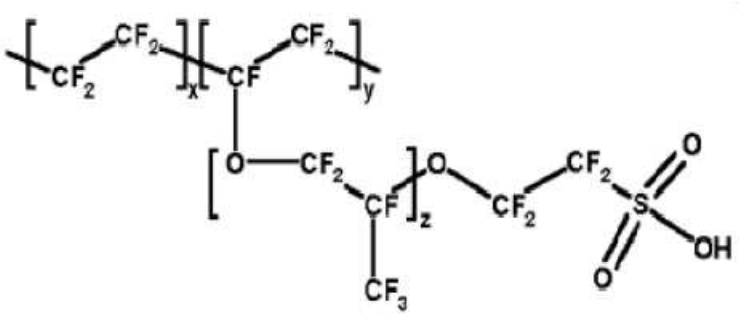

Figure 3. Molecular structure of Nafion (Gleason et al., 2008).

The sulfonic acid-water association is necessary for the celebrated proton transport of Nafion. Hence, an increase in the number of sulfonic acid groups can, in principle, help to enhance the water content in the membranes (Pillai, 2008). However, at high temperatures (>100°C) the sulfonic groups start decomposing, thus reducing the stability of Nafion structure and the electrical conductivity of the membranes (Liu et al., 2010).

Apart from possessing high cost, the main disadvantage of Nafion membrane lies in its long-term durability. The durability characteristic of the membrane is adversely affected by a large quantities of water adsorbed during start-up and shutdown sequences of PEMFCs. Due to Nafion sensitivity to water, the alternating swelling and contraction cycles originated from excessive water can gradually lead to destruction of the membrane (Gleason et al., 2008).

Additionally, a high concentration of sulfonic acid groups in Nafion compromises the polymer's mechanical strength, thus an ideal equivalent weight of Nafion is required (Hickner et al., 2004).

1.4. Carbon Nanotubes & Polyvinyl Alcohols

Carbon nanotubes, allotropes of carbon with a cylindrical nanostructure, classified as a new class of advanced nanomaterials capable of imparting electrical conductivity into Nafion. Carbon nanotubes (CNTs) reinforced Nafion composite membranes have shown competitive advantage over commercial Nafion products in mechanical stability (Liu et al., 2006). Mutiwalled CNTs/Nafion hybrids have also exhibited favorable indications over pristine Nafion in membrane proton conductivity (Liu et al., 2010). However, carbon nanotubes are difficult to process and insoluble in most solvents. Recently, modifications of multiwalled carbon nanotubes (MWCNTs) using various reactive as well as non-reactive polymers have extensively been investigated (Liu et al., 2009 and Chen et al., 2008).

Polyvinyl alcohol (PVA), monomer formula C_2H_4O, is a water-soluble synthetic polymer. PVA has excellent film forming, emulsifying, and adhesive properties. It also has high tensile strength, flexibility, high oxygen and aroma barrier, although these properties are dependent on humidity. PVA decomposes rapidly above 200°C as it undergoes pyrolysis (Polyvinyl alcohol MSDS, 2008). PVA is often synthesized from a polyvinyl ester called polyvinyl acetate (PVAc) (Figure 4).

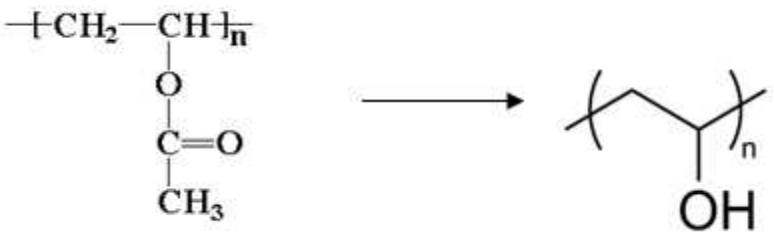

Figure 4. Synthesis of PVA from PVAc.

1.5. Goals of This Study

The objective of this project is to experimentally compare the performance in mechanical strength and electrical conductivity of MWCNT-PVA/Nafion membranes with commercial Nafion 212 and recast Nafion. The hypothesis of the work presented in this report was that composite membranes can demonstrate better mechanical stability than both pristine Nafion and Nafion 212 without affecting their proton conductivity. Firstly, polyvinyl alcohols were used to synthesize CNT-PVA hybrids using ozone mediated process. Fourier transform infrared spectroscopy, thermogravimetric analysis, X-ray photoelectron spectroscopy, and solubility test were used to verify the attachment of PVA onto the surface of MWCNT. Secondly, CNT-PVA/Nafion composite membranes were prepared, and then characterized using various measurements such as mechanical properties and electrical conductivity.

Chapter 2. LITERATURE REVIEW

2.1. Beneficial Effects of CNTs on Performances of Nafion Membranes

Recent researches on PEMFCs have focused on overcoming the major drawbacks of Nafion membranes. Two common approaches were discussed to tackle this problem: the first one consisted of replacing Nafion by alternative polymers; the second strategy relied on modification of Nafion with inorganic fillers. The main reason for adding inorganic substances was to enhance water retention at high temperatures and mechanical properties of the membranes while keeping the ionic conductivity as high as possible (Thomassin, 2007).

In 2006, a group of scientists at Chinese Academy of Sciences in Beijing developed a carbon nanotubes (CNTs) reinforced Nafion composite membrane for the H_2/O_2 fuel cell. Ball-milling method was utilized to obtain high shear mixing necessary to disentangle mutiwalled CNTs and dispersed them uniformly in a Nafion matrix (Liu et al., 2006). An addition of a small amount of 1 wt% CNTs in Nafion excellently improved the mechanical property of the composite membrane. The strength of Nafion membrane modified by CNTs increased by 68.8% and 28.7% compared with that of recast Nafion and commercial Nafion NRE-212, respectively (Table 1).

Table 1. Comparison of maximum strength of Nafion membranes (Liu et al., 2006).

Membrane	Recast Nafion	Nafion NRE-212	1 wt% CNTs/Nafion	1 wt% Carbon black/Nafion	PTFE/Nafion
Thickness (mm)	0.050	0.050	0.050	0.050	0.050
Maximum strength (MPa)	22.08	28.97	37.28	20.13	41.1

At the same time, there was no obvious difference in the open-circuit voltage (OCV) as well as overall single cell performance of Nafion NRE-212 and CNTs/Nafion (Figure 5). Therefore, it can be concluded that CNTs acted only as filbril-reinforced functions which did not cause short-circuit, as opposed to forming a continuous electron transfer channel (Liu et al., 2006).

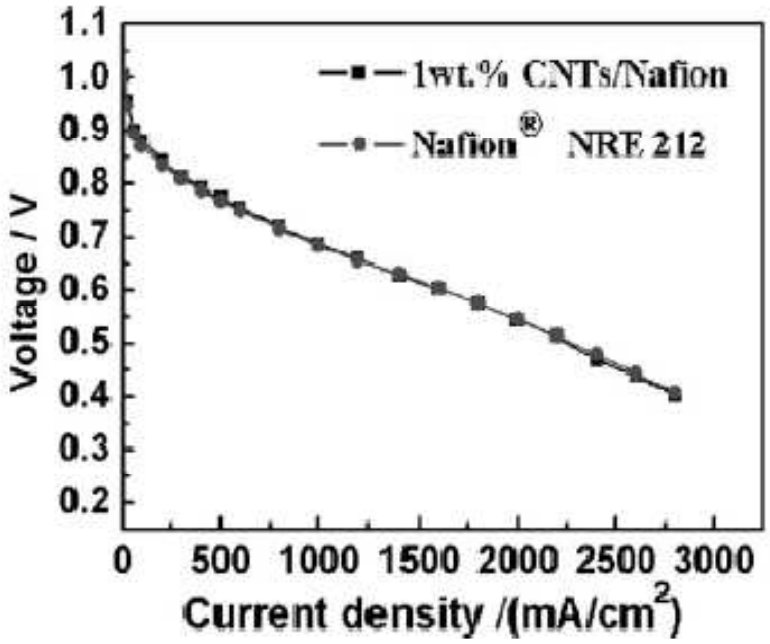

Figure 5. Comparison in performance of H_2/O_2 cell with 50μm thick CNTs/Nafion composite membrane and Nafion NRE-212 membrane (Liu et al., 2006).

Pillai et al., (2008) reported a chemical strategy to increase the sulfonic acid content of Nafion membranes by incorporating sulfonic acid functionalized single-walled carbon nanotubes (S-SWCNTs) and demonstrated its remarkable utility as electrolyte in PEMFC applications. Their finding showed a significant improvement in temperature-dependent ionic conductivity of Nafion/S-SWCNT composite membrane over commercial Nafion-1135. Figure 6 revealed an

almost one order of magnitude higher conductivity for the composite than that of Nafion-1135 (Pillai et al., 2008).

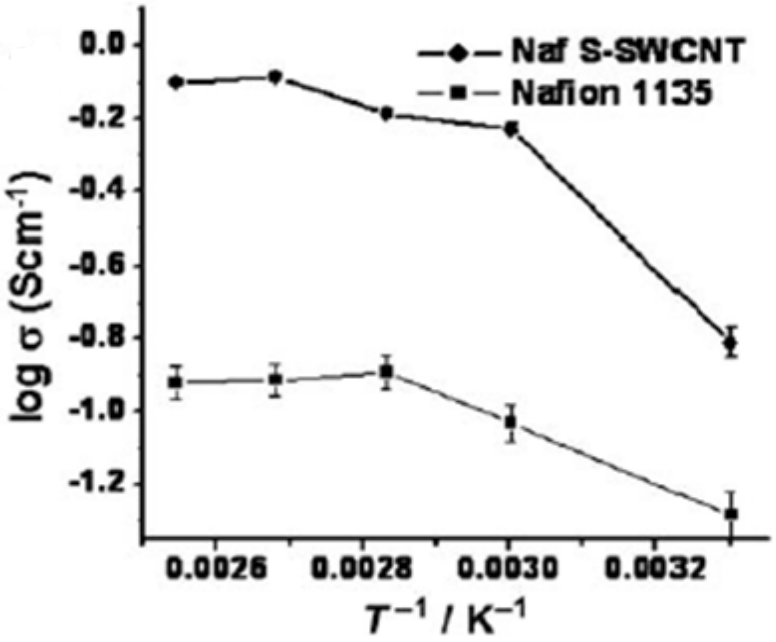

Figure 6. Comparison of proton conductivity of Nafion-1135 and Nafion/S-SWCNT at 100% relative humidity in the range of 1 MHz to 0.1 Hz (Pillai et al., 2008).

The conductivity values were 0.0155 S/cm and 0.0101 S/cm for composite membrane and Nafion-1135, respectively, thus the enhanced conductivity could be attributed solely to the membrane. Additionally, a decrease in electrolyte resistance of Nafion membrane incorporating S-SWCNTs in comparison with that of Nafion-1135 was noticed (Figure 7). Although the OCV obtained for composite membrane was lower than that for Nafion-1135 (0.9V of Nafion/S-SWCNT vs. 0.96V of Nafion-1135, both at 60°C), the activation loss and ohmic loss of the composite membrane were considerably lower than those of Nafion-1135 (Figure 8).

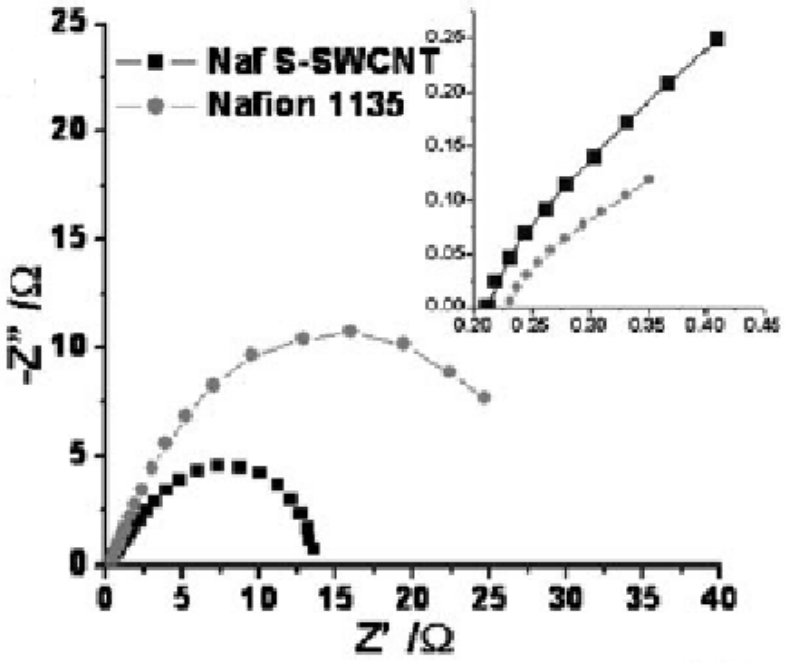

Figure 7. Nyquist impedance (Z) plots for MEAs made with Nafion-1135 and Nafion/S-SWCNT membranes. The measurements were carried out at room temperature with a flow of humidified H_2 and O_2. The MEAs were fabricated using 20% Pt/C catalyst for both anode and cathode in a single cell experiment (Pillai et al., 2008).

Figure 7 illustrated that the electrical impedance of modified S-SWCNT/Nafion membrane was one third of that of Nafion-1135, thus it was reasonably deducted that Nafion/S-SWCNT membrane would demonstrate greater proton conductivity.

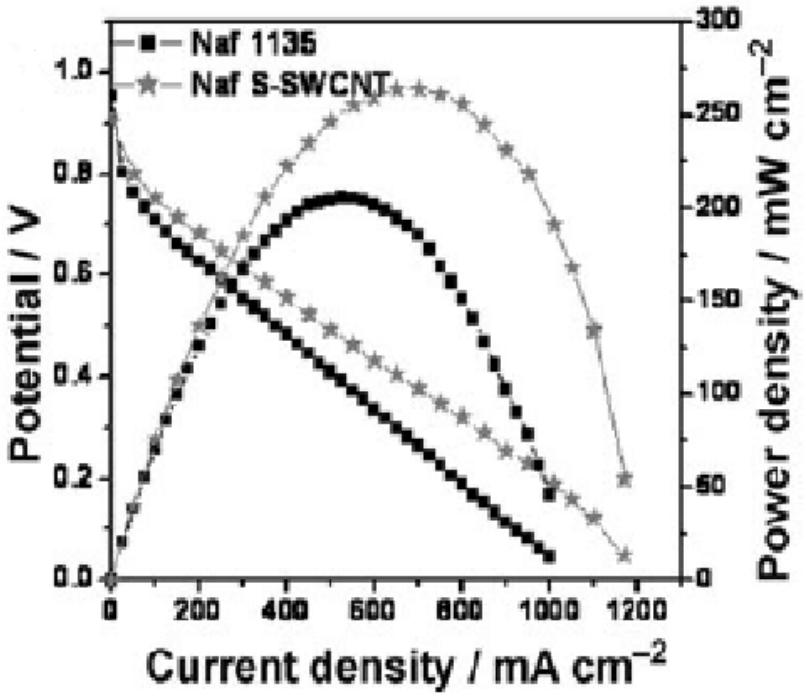

Figure 8. Polarization curves obtained with Nafion/S-SWCNT and Nafion-1135 membranes at 60°C with humidified H_2 and O_2 (flow rate 0.4 slpm). The cells were conditioned for 30 min at open-circuit potential and at 0.2V for 15 min before measurements. The MEAs were fabricated using 20% Pt/C catalyst for both anode and cathode in a single cell experiment (Pillai et al., 2008).

In Figure 8, the Nafion/S-SWCNT membrane gave a maximum power density of 260 mW/cm^2 at 0.42 V, whereas the Nafion-1135 membrane gave 210 mW/cm^2 at 0.39 V (Pillai et al., 2008).

Pillai et al., (2010) also opened up a new pathway to systematically tune the properties of polymer electrolytes using appropriately functionalized CNTs fabricated on other membrane materials rather than Nafion. The success of the accomplishment through preparation of novel phosphonic-acid (PA) functionalized CNTs (p-CNTs) and their composite with PA-doped polybenzimidazole (PBI) membranes (PBpNT) was reported. The proton conductivity of the bare (PBI iso) and composite membranes after doping with PA was 0.07 and 0.11 S/cm, respectively, suggesting almost half of an order of magnitude of improvement (Figure 9).

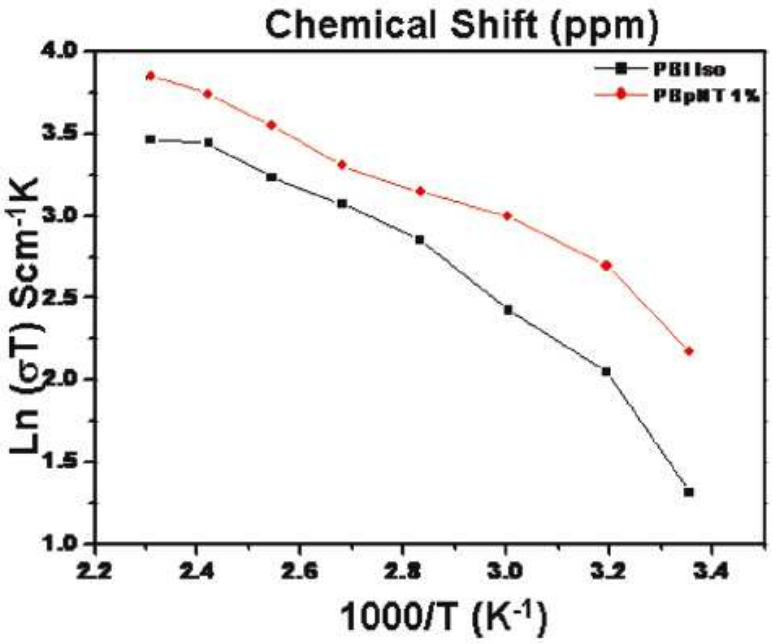

Figure 9. Arrhenius plot for the proton conduction of PBI iso and PBpNT membranes from 25 to 160°C through two-probe impedance measurements (Pillai et al., 2010).

An enhancement of 40% in power density of PBpNT compared to that of PBI iso proved that the composite membrane exhibited better cell performance. For example, at 0.6 V, PBpNT gave a current density of 625 mA/cm^2, while PBI bare membrane gave only 400 mA/cm^2 (Figure 10). Furthermore, the maximum power density of PBpNT was 780 while that of PBI iso was 600 mW/cm^2 (Pillai et al., 2010).

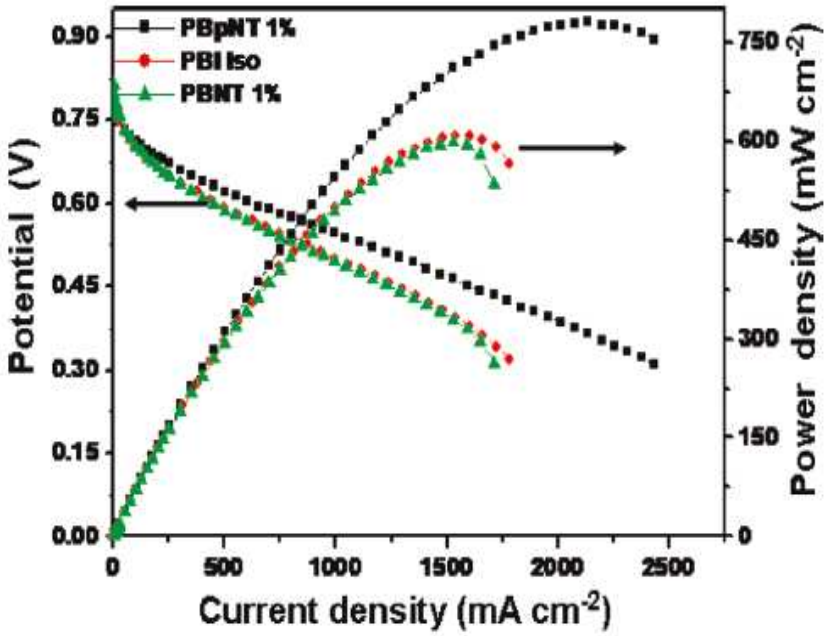

Figure 10. Polarization plots of PBI iso, PBpNT, and PBNT composite membranes measured at 140°C by passing dry H_2 and O_2 at flow rate of 0.2slpm. The cells were conditioned at 0.6 V for 30 min.

The mechanical stability of the membrane was also significantly improved by the addition of p-CNTs. The composite membrane possessed yield strength of 75 MPa compared to 62 MPa of the pristine membrane, suggesting its remarkable ability to retain its behavior even at higher stress (Figure 11). Further, ultimate strengths of 100 MPa and 65 MPa for the BPpNT 1% composite and pristine PBI, respectively, showed comparative advantage of composite membranes (Pillai et al., 2010).

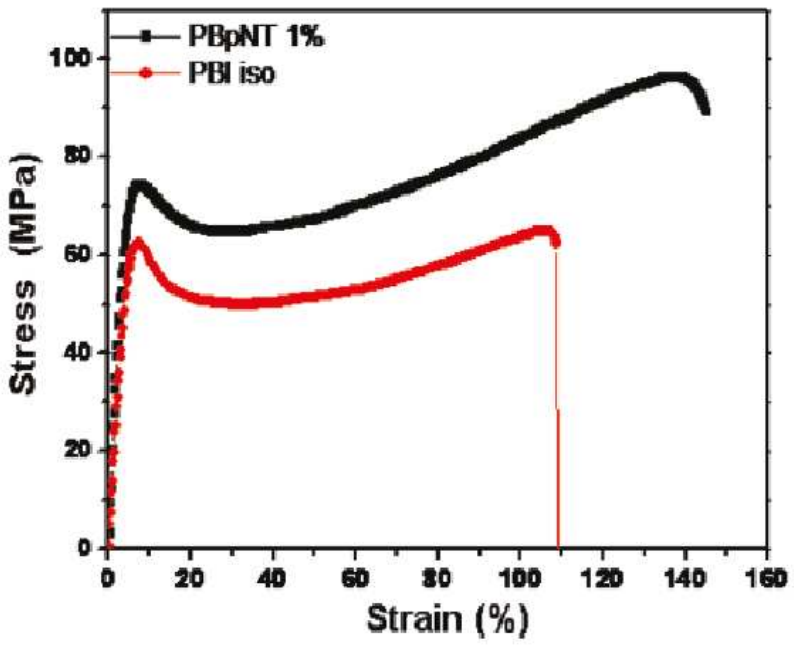

Figure 11. Stress-strain curve for pristine PBI and PBpNT composite membrane (Pillai et al., 2010).

2.2. Previous Research at R&D Center for Membrane Technology in Chung Yuan Christian University (CYCU)

Liu et al., (2008) reported their first attempt to extend the scope of CNT applications by modifying CNTs with a commercial engineering plastic called poly(2,6-dimethyl-1,4-phenylene oxide) (PPO). Their approach was to prepare CNT-PPO using brominated PPO under the condition of atom transfer radical polymerization (Figure 12). Successful formation of PPO-functionalized-CNT was confirmed by Raman spectroscopy, FTIR-ATR spectra, and thermal analysis (Liu et al., 2008).

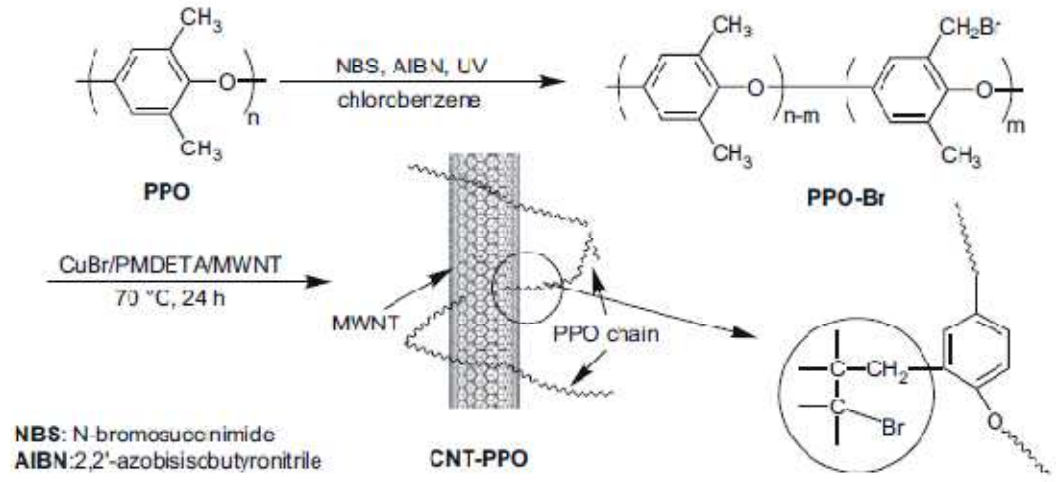

Figure 12. Synthesis route of PPO-modified carbon nanotubes (Liu et al., 2008).

Liu and Chang (2009) made a breakthrough in direct functionalization of CNTs using ozone-mediated process for the preparation of a wide range of high performance polymer/CNT composites. In this research, four polymers – poly(vinylidene fluoride) (PVDF), polysulfone (PSF), poly(2,6-dimethylphenylene oxide) (PPO), and poly(phthalazinone ether ketone) (PPEK) - were chemically bonded to MWCNTs. The mechanism behind this method was the generation of free radical groups such as alkylperoxide and hydroperoxide under heat, which were reactive toward the sp^2 hybrid carbons of CNTs, leading to the interactions between CNT sidewalls and the radicals of polymer chains from decomposition of peroxide groups (Figure 13).

High Resolution Transmission Electron Microscopy (HRTEM) was used to characterize polymer-functionalized MWCNTs (Figure 14). Pristine CNTs showed layered bundles without covering with amorphous carbon. For all polymer-functionalized CNTs, amorphous polymer layers covering on the outer bundles of MWCNTs were observed, affirming the presence of polymers on CNTs surface. The thickness of the polymer layer was about 2 – 5 nm (Liu and Chang, 2009).

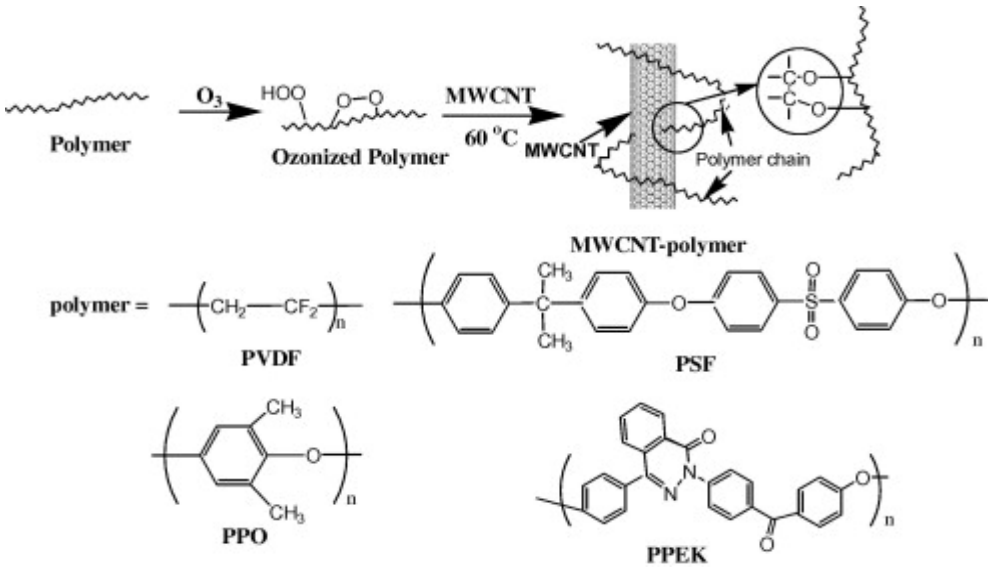

Figure 13. Ozone-mediated functionalization of MWCNTs with polymers (Liu & Chang, 2009).

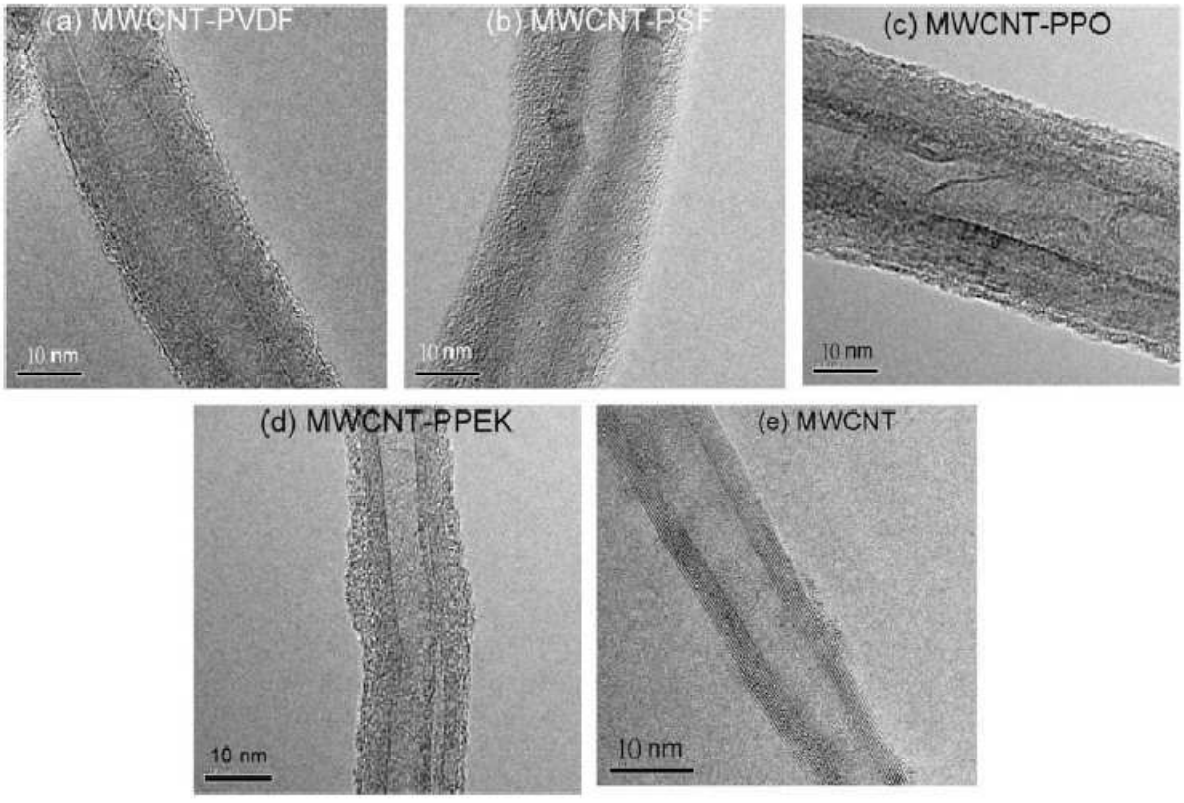

Figure 14. HR-TEM micrographs of MWCNT-polymer hybrid materials (Liu & Chang, 2009).

One common problem of using CNTs to modify PEMs is the risk of short-circuiting caused by the electrical conductivity of CNTs. By keeping the CNT contents below the percolation threshold of 1 wt%, the modified membrane showed improvement in mechanical properties without a significant drop in proton conductivity (Liu et al., 2006). Addition of 2 wt% carboxylic acid-functionalized MWCNTs was used to enhance the dispersion ability of CNTs to Nafion-based membranes, thus increase their Young's modulus by 160% (Thomassin et al., 2007). Pillai's follow-up work using sulfonated MWCNTs (S-MWCNTs) to modify Nafion also found out that the optimum loading of S-MWCNT to the Nafion membranes was 0.05 wt% (Pillai et al., 2009).

In 2010, Liu and his group continued investigating another option using Nafion-functionalized MWCNTs for Nafion membranes. This functionalization was based on the radical addition reaction between the MWCNT surfaces and the radicals of ozone-treated Nafion chains. Four different kinds of composite membranes were prepared: 0.025 wt% of Nafion-CNTs incorporated to Nafion (N/MN-0.025), 0.05 wt% of Nafion-CNTs incorporated to Nafion (N/MN-0.05), 0.1 wt% of Nafion-CNTs incorporated to Nafion (N/MN-0.1), and 0.2 wt% of Nafion-CNTs incorporated to Nafion (N/MN-0.2) (Liu et al., 2010). The CNT-Nafion loading consisted of high compatibility with the Nafion matrix, thus Nafion membranes with CNT-Nafion additives exhibited improved mechanical properties in comparison with pristine Nafion (Figure 15). The tensile strength and Young's modulus of N/MN-0.05 were 16 MPa and 158 MPa, respectively, which were about 1.5-times the values measured with pristine Nafion. The increased mechanical strength associated with MWCNT-Nafion reinforcement could reduce the failure of membranes operating in hydrated states (Liu et al., 2010).

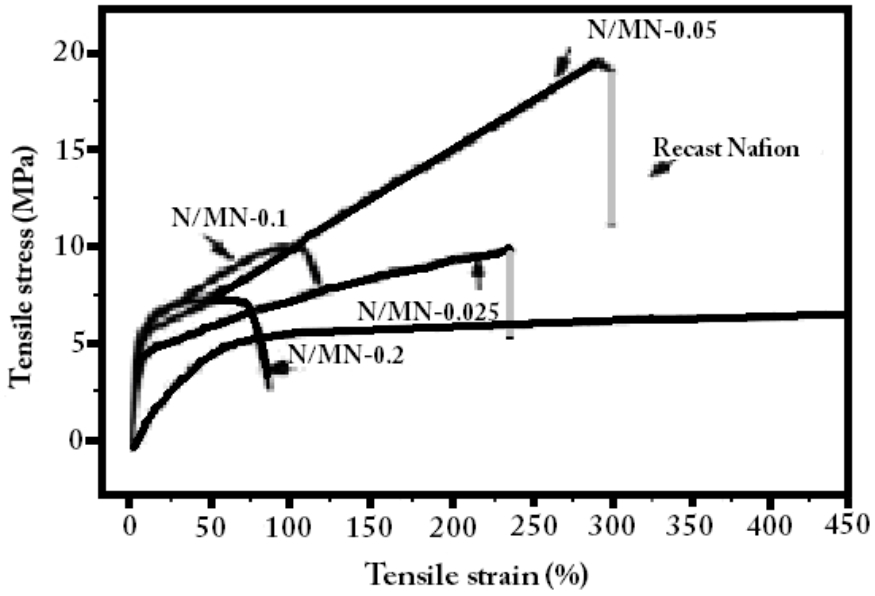

Figure 15. Strain-stress curves of recast Nafion membrane and N/MN composite membranes (Liu et al., 2010).

All of the produced N/MN composite membranes showed proton conductivity comparable or even higher than that of recast Nafion membrane, with N/MN-0.05 having relatively highest conductivity (Figure 16). For example, at 80°C, the proton conductivity of N/MN-0.05 was measured to be 0.112 S/cm, which was about five-fold increase from that of recast Nafion (0.02 S/cm at 60°C) and was about three-times of that measured with commercial Nafion 212 (0.04 S/cm) (Liu et al., 2010).

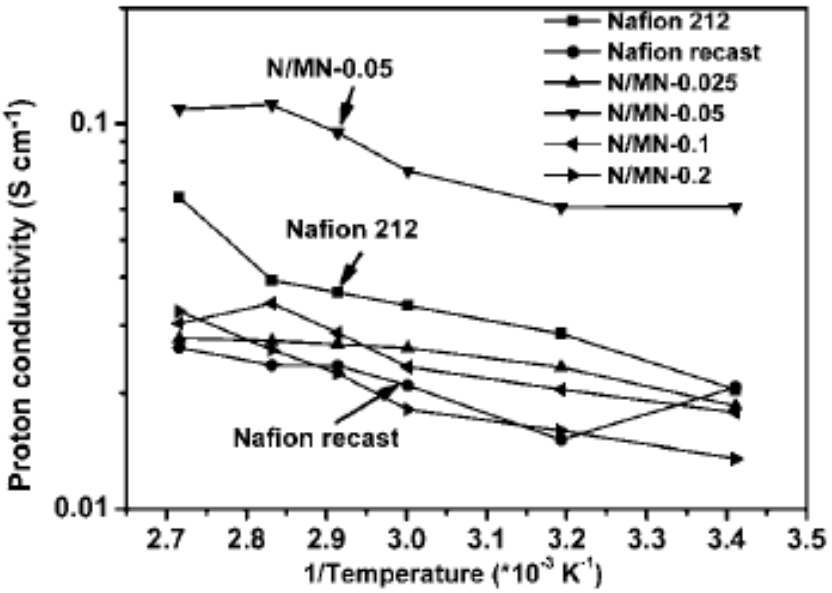

Figure 16. Temperature-dependent proton conductivity of recast Nafion and N/MN composite membranes (Liu et al., 2010).

In a single cell test, while all other composite membranes did not exhibit as good a performance as did commercial membrane, the high performance of N/MN-0.05 was noteworthy. The current densities measured for N/MN-0.05 at potential of 0.6 V and 0.4 V were 1556 mA/cm^2 and 966 mA/cm^2, respectively. These values were about 1.5-times higher than those of pristine membrane (Figure 17). Correspondingly, N/MN-0.5 membrane gave a maximum power density of 650 mW/cm^2 at 0.50 V, while pristine Nafion membrane showed 451 mW/cm^2 at 0.47 V using the same MEAs setup (Figure 18).

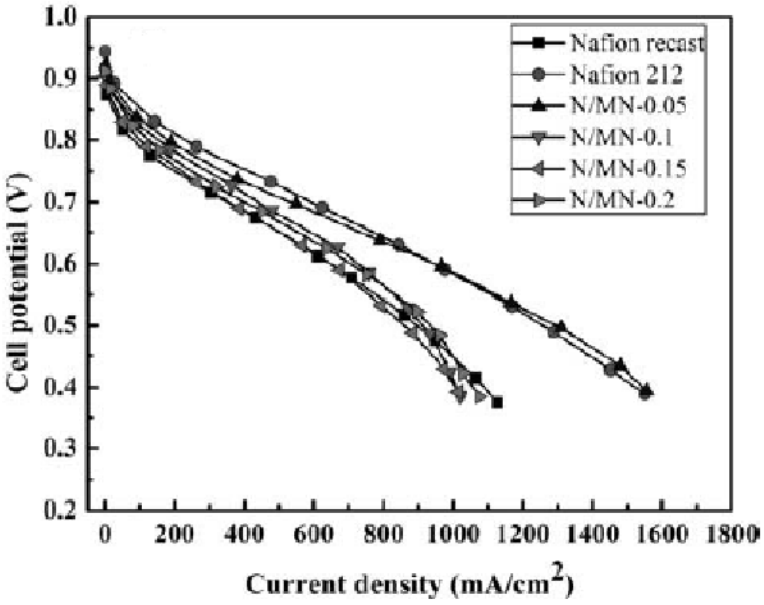

Figure 17. Current density vs. Cell potential of commercial membrane, composite membranes and recast membrane (Liu et al., 2010).

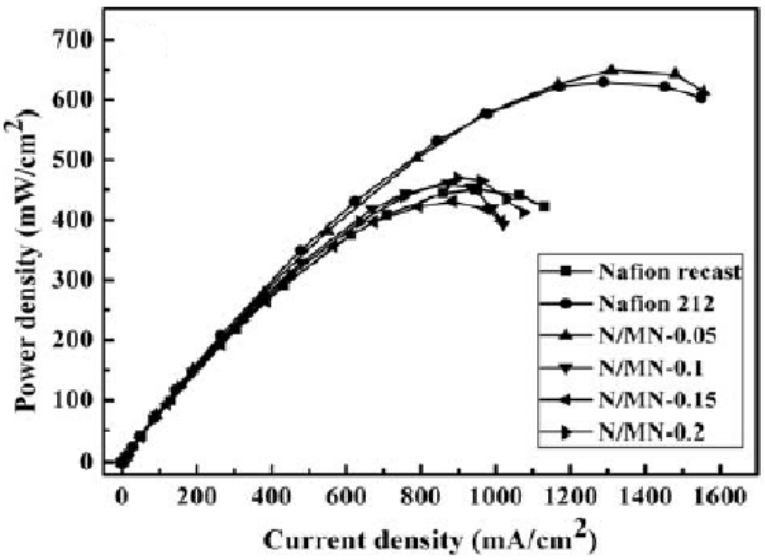

Figure 18. Power density vs. Current density of composite membranes, commercial membrane, and recast membrane (Liu et al., 2010).

Chapter 3. EXPERIMENTAL METHODS

3.1. Modification of MWCNTs with PVA via Ozone Treatment

Ozone appears to be an effective agent for the modification of polymers and other materials. Ozone-mediated approach was discovered in 2009 by Professor Liu's group as a convenient way to functionalize CNTs using unmodified MWCNTs and non-reactive polymer chains. Compared to previous "grafting from" or "grafting to" methods, ozone treatment has proved to show the ability to functionalize pristine CNTs with a wide range of polymers, including commercially available engineering plastics (Liu et al., 2009).

3.1.1. Preparation of Polyvinyl Alcohol solution

Polyvinyl alcohol (PVA, Aldrich Chemical Company Inc., USA) was chemically bonded to MWCNTs (average diameters of 10-50 nm and length of 1-25 μm, obtained from Carbon Nanotube Co., Ltd., Incheon, Korea) through an ozone-mediated process. 1 gram of PVA was completely dissolved in 35 ml of water at 70°C to form an aqueous solution. The PVA solution was then placed in a 100-ml flask. A continuous stream of O_3/O_2 mixture (flow rate 6 L/min; concentration 28 g/m^3) which was generated by an ozone generator (Ozone Group, Taiwan) bubbled through the solution at room temperature for 15 minutes. In a similar manner, a pure stream of argon gas was used to purge through the solution for 15 minutes to remove excess free peroxide groups.

3.1.2. CNT-PVA solution

After 0.5 gram CNT was quickly added in the solution (Figure 19), the mixture was stirred at 80°C to react for 3 hours.

Figure 19. CNT-PVA black-colored solution.

3.1.3. Collecting CNT-PVA from the solution using centrifuge

Centrifugal machine EBA 21, manufactured by international Hettich group (Japan), was employed to extract concentrated CNT-PVA from CNT-PVA solution. The higher the rotational speed was, the better separation could be obtained for a given smaller volume.

Using the driving force of the centrifuge (maximum speed 6000 rpm) to separate CNT-PVA from the solvent, the CNT-PVA in solid was collected at the bottom of the tubes (Figure 20). The remaining solution was clear since there was little or no CNT left.

Figure 20. Solid-formed CNT-PVA collected.

3.1.4. Purifying CNT-PVA

In order to remove more solvent and excess PVA, CNT-PVA was filtered and washed with tetrahydrofuran THF (Figure 21). A special type of filtered membrane, product of Critical Process Filtration Inc. in USA, was used during the filtration process. The membrane has pore size of 0.2 µm and diameter of 47 mm (Figure 22). The membrane was pre-treated using THF to prevent it from being torn up. The filtered CNT-PVA can be seen in Figure 23. The collected CNT-PVA was then dried under vacuum overnight.

Figure 21. Filtration method setup and Tetrahydroduran in the background.

Figure 22. Membrane filter box (on the left) and membrane close-up view (on the right).

Figure 23. Collected CNT-PVA after filtration.

Figure 24 shows the final product of the incorporation of PVA into MWCNTs. The weight of this sample was found to be 0.4 grams.

Figure 24. Powdered PVA-modified-MWCNTs.

3.2. Verifying Successful Synthesis of CNT-PVA

3.2.1. Fourier Transform Infrared Spectroscopy

Fourier Transform Infrared Spectroscopy (FTIR) is a useful analysis tool using mid-infrared radiation with wavenumber $\bar{\nu}$ in the range of 4000 and 670 cm^{-1} (frequency ν from 1.2 x 10^{14} to 2.0 x 10^{13} Hz). The working mechanism of FTIR is understood as: when a light beam emitted from FTIR interacts with the sample, the infrared radiation energy of that light excites atoms existing inside the sample, thus stimulate vibration motion of chemical bonds in the sample. Since functional groups absorb infrared radiation at the same wavenumber range regardless of different molecular structure, a relationship between an infrared band spectrum and a chemical structure can be found, providing various information about an unknown entity (Skoog, 1998).

Table 2. Correlation between organic groups and peaks frequencies and intensities in FTIR (Skoog, 1998).

Bond	Type of compound	Frequency range (cm^{-1})	Intensity
C – H	Alkanes	2850 – 2970	Strong
		1340 – 1470	Strong
C – H	Alkenes	3010 – 3095	Medium
		675 – 995	Strong
C – H	Alkynes	3300	Strong
C – H	Aromatic rings	3010 – 3100	Medium
		690 – 900	Strong
O – H	Monomeric alcohols, phenols	3590 – 3650	Variable
	Hydrogen-bonded alcohols, phenols	3200 – 3600	Variable, broad
	Monomeric carboxylic acids	3500 – 3650	Medium
	Hydrogen-bonded carboxylic acids	2500 – 2700	Broad

N – H	Amides, amines	3300 – 3500	Medium
C = C	Alkenes	1610 – 1680	Variable
C = C	Aromatic rings	1500 –1600	Variable
C≡ C	Alkynes	2100 – 2260	Variable
C – N	Amides, amines	1180 –1360	Strong
C≡ N	Nitriles	2210 – 2280	Strong
C – O	Alcohols, ethers, carboxylic acids, esters	1050 – 1300	Strong
C = O	Aldehydes, ketones, carboxylic acids, esters	1690 – 1760	Strong
NO_2	Nitro compounds	1500 – 1570 1300 – 1370	Strong Strong

In this project, FTIR was used to qualitatively determine the chemical structure of PVA-modified MWCNTs. FTIR spectra were obtained through the attenuated total reflectance method using a Perkin Elmer Spectrum One FTIR equipped with a multiple internal reflectance apparatus and a ZnSe prism as an internal reflection element. A milligram of finely ground CNT-PVA was mixed with 100 mg of dried potassium bromide powder. Mixing was carried out with a mortar and a pestle (Figure 25). The mixture was then pressed in a special die at about 400 kg-f/cm^2 (Figure 26 and Figure 27) to form a transparent disk (Figure 28). The disk was held in the instrument beam for spectroscopic examination (Figure 29). Note that appropriate proportions of KBr and CNT-PVA were needed to make sure that neither was transmittance too low nor were characteristic peaks unclear.

Figure 25. Finely grounded mixture of CNT-PVA and KBr in a mortar.

Figure 26. Special die (on the right) and spectrum sample holder (on the left).

Figure 27. Standard press with capacity of 1000 kg-f/cm^2.

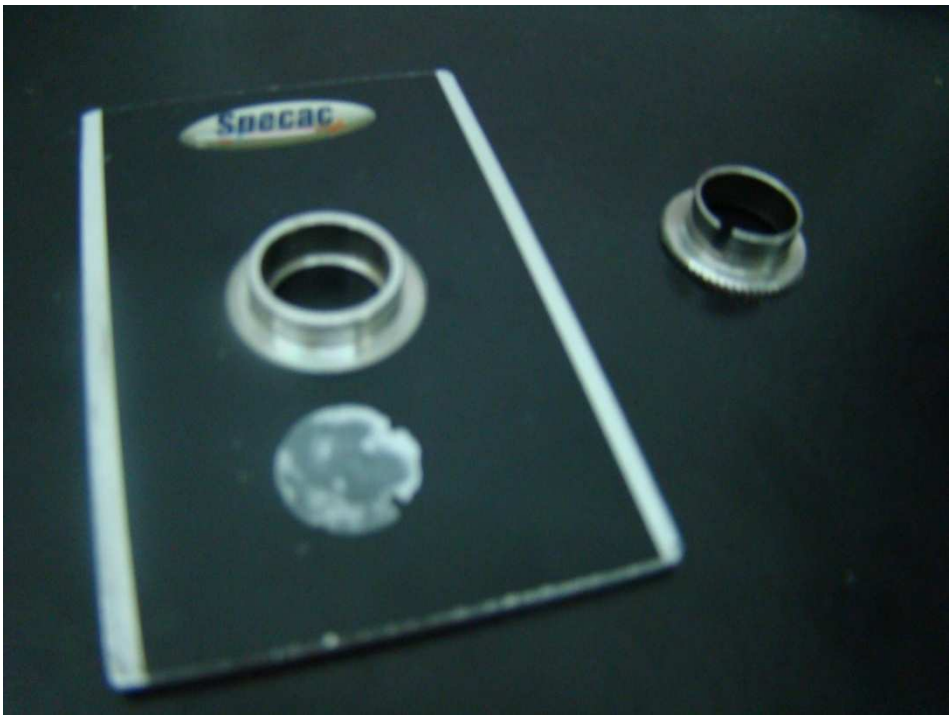

Figure 28. A transparent disk of CNT-PVA/KBr on Specac.

Figure 29. FTIR spectroscopy setup (light beam pass through the circular hole on the spectrum sample holder).

3.2.2. Thermogravimetric Analysis

Thermogravimetric analysis (TGA) was performed with an instrument from Thermal Analysis Incorporation (TA-TGA Q-500) under inert nitrogen atmosphere (Figure 30).

Figure 30. Thermogravimetric Analysis Instrument TGA Q500.

TGA based on continuous measurements of the sample weight on a sensitive thermobalance as the sample temperature was increased in air or inert atmosphere. TGA was employed to determine the characteristics as well as to test the thermal stability of CNT-PVA. A small amount (> 2 mg) of powder CNT-PVA was placed in a high-precision balance platinum pan. The sample was then loaded into an electrically heated oven attached with a thermocouple to accurately measure the temperatures (Figure 31). The atmosphere was purged with nitrogen to prevent oxidation and other undesired reactions. Using TA analysis software control menu,

"Jump to 110°C" and "Isothermal for 15 min" were selected to remove moisture from the sample. After sample temperature was cooled back down to room temperature (< 50°C), "Ramp 10°C/min to 900°C" control mode was set. The TA analysis collected the data and generated plots of weight percent vs. temperature of CNT-PVA.

Similar procedures were repeated with pure CNT and pure MWCNTs, in which a sample of each weighing 2 – 5 mg was prepared.

Figure 31. Sample contained in the Platinum pan being loaded into the electrically heated oven.

3.2.3. X-ray Photoelectron Spectroscopy Analysis

X-ray photoelectron analysis (XPS) was conducted with a K-Alpha manufactured by Thermo Scientific, U.S.A using an X-ray as the radiation source (Figure 32).

Figure 32. XPS machine and its three guns.

X-ray gun (maximum energy of 1486.6eV) attacked the electron on the innermost 1s orbital of an atom, thus forced it out of the atomic orbit. The kinetic energy consumed was then measured and corresponding binding energy between atoms was calculated. The peak position, the numbers of peaks, as well as their height further characterize the modification of CNT on MWCNTs surface.

3.2.4. Solubility Test

Small amount of powder CNT-PVA and pure powder MWCNTs were both dissolved in water, and then placed in an E-120H Elmasonic for an hour to obtain well-mixed dispersion (Figure 33). After taking samples out of the ultrasonic, the separation between solute and solvent in each bottle was observed and pictures were taken for comparison.

Figure 33. Elmasonic E-120H model manufactured by Elma Ultrasonics in Germany.

3.3. Fabrication of CNT-PVA/Nafion Composite Membranes

3.3.1. Functionalization of CNT-PVA with Nafion

1.5 mg of CNT-PVA was diluted in a solvent mixture of 1.5 ml Isopropyl Alcohol (IPA, Echo Co., U.S.A) and 1.5 ml water to form a 0.5M CNT-PVA solution (Figure 34).

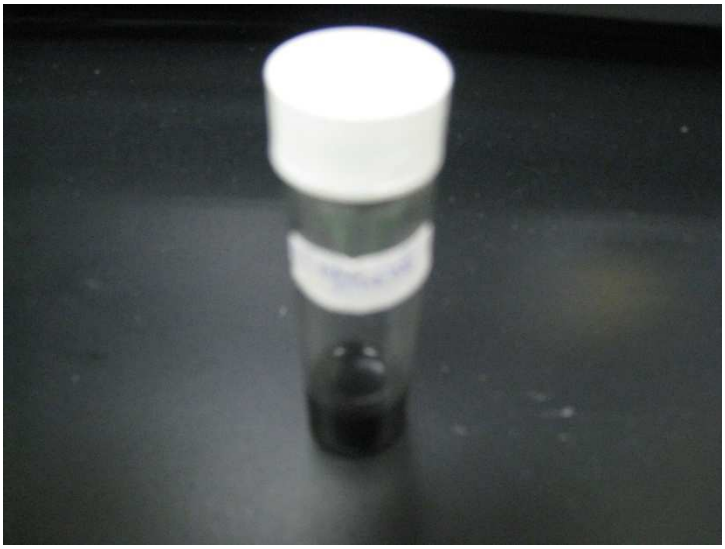

Figure 34. Powder CNT-PVA diluted in IPA/H_2O solution.

The solution was then thoroughly dispersed using an Elmasonic LC30 (Elma Ultrasonics, Germany). Meanwhile, 1.5 gram of Nafion® D2020 (DuPont, U.S.A) was diluted in a mixture of 1.5 g of IPA and 1.5 g of water to decrease the viscosity of the Nafion solution. CNT-PVA solution was then added into the Nafion solution by the amounts shown in Table 3 to yield three different desired concentrations of CNT-PVA/Nafion mixture.

Table 3. Solution ratio in mixture needed to make three kinds of modified membranes.

Weight percent (%)	Nafion solution (g)	CNT-PVA solution (mg)
0	0.3	0
0.05	0.3	0.15
0.1	0.3	0.3

Three mixtures were stirred using magnets (Figure 35) and sonificated for two hours to make sure that CNT-PVA solution was well incorporated into Nafion matrix.

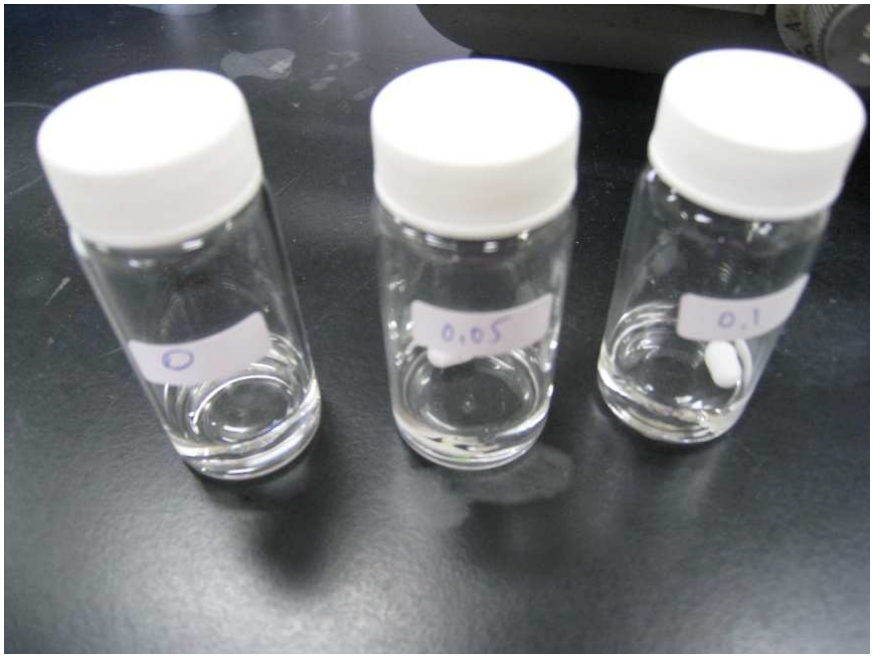

Figure 35. Images of 3 different CNT-PVA/Nafion mixtures.

All of the above solutions were poured into Petri dishes, each with diameter of 9 centimeters, to obtain appropriate membrane thickness. Petri dishes containing CNT-PVA/Nafion solutions inside were put in a drying oven set at 50°C overnight. Next morning, the temperature of the oven was reset at 130°C for an hour and then 150°C for another hour. This step was called "membrane annealing" in order to increase the membrane mechanical strength.

3.3.2. Acidification of membranes

Commercial proton-exchanged membrane Nafion® 212 purchased from DuPont Fluoroproducts was used along with three successfully fabricated membranes for acidification. All membranes were put in a 1000-ml glass beaker containing boiling water for 40 minutes. A glass funnel was used to prevent membranes from floating on the surface, in other word, to keep them completely immersed in water. The membranes were then boiled in 10 wt% H_2O_2 (product

of SHOWA Corp., Japan) at 80°C for an hour to remove organic substances and other impurities on the surface of the membranes. Accordingly, the membranes were boiled in water at 100°C for another 40 minutes. The process continued with boiling membranes in 1M H_2SO_4 at 80°C for one hour, and in boiling water for 40 minutes. Notice that glass material was used instead of any metals since transitional metals can catalyze H_2O_2 decomposition. Finally, all membranes were taken out then put in drying oven at a temperature of 50°C overnight (Figure 36).

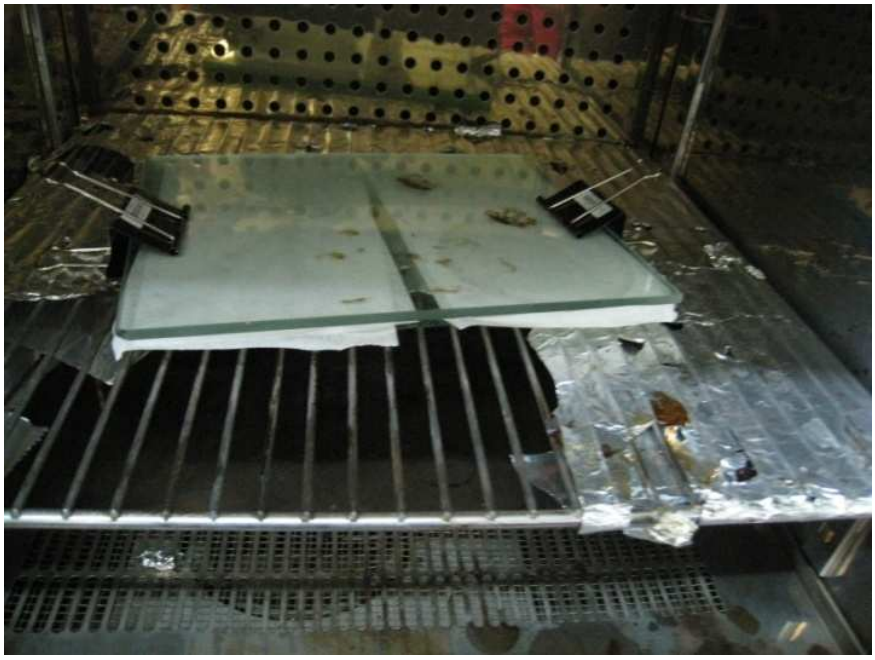

Figure 36. Acidified membranes put in drying oven overnight.

Figure 37 shows the fabricated membranes after taking out of the oven.

Figure 37. Fabricated membranes – upper left: 0.1 wt% CNT-PVA/Nafion; upper right: recast Nafion; lower left: 0.05 wt% CNT-PVA/Nafion; lower right: commercial Nafion® 212.

3.4. Characterization of CNT-PVA/Nafion Composite Membranes

3.4.1. Instron Test

The mechanical properties of CNT-PVA/Nafion composite membranes were analyzed with an Instron 5543 analyzer (Instron Corp., U.S.A) at an elongation rate of 0.5 mm/min (Figure 38). Strips of membranes with dimension of 0.5 cm width and 4 cm length were prepared. The thickness of each membrane was measured (Figure 39) and so were the width of the membrane and the length of the membrane held between two clamps of the Instron (Figure 40).

Figure 38. Instron 5543 analyzer.

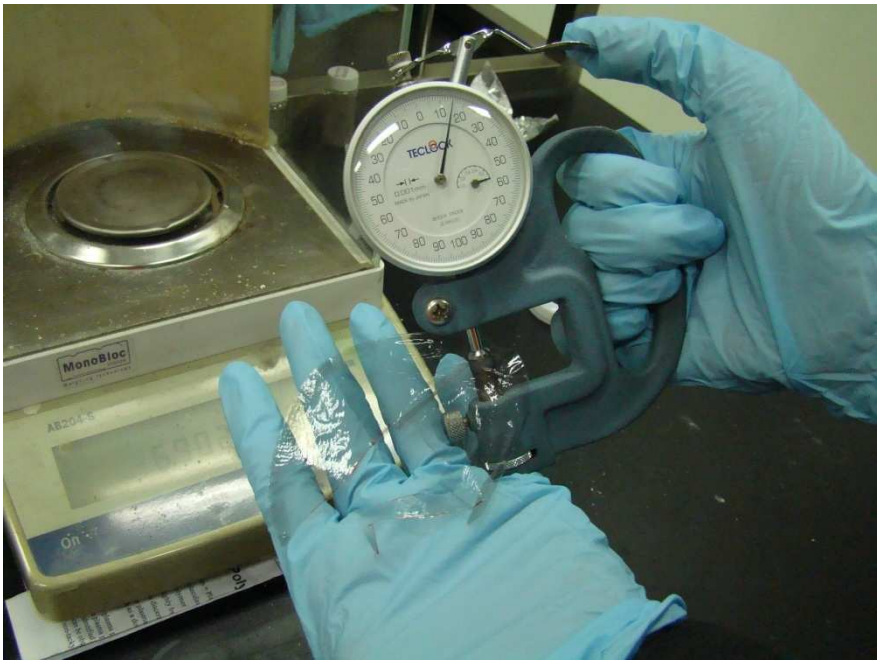

Figure 39. Measuring the thickness of membrane.

Figure 40. Measuring the length of membrane between two Instron clamps.

Instron analyzer applied a force on the membrane strip to elongate the strip until it was broken. The fatigue point provided information about membrane maximum stress and maximum strain while the slope of stress vs. strain graph generated an average Young modulus number.

3.4.2. Conductivity Test

The ac electrical conductivity was measured with a Solartron SI-1287 Electrochemical Interface equipped with a Solartron 1255B Frequency Response Analyzer at a frequency range of 0.1 Hz to 1 MHz. This instrument is a product of AMETEK, Inc. in U.K. A package of software named Zplot and Zview came with the connected computer. Conductivity value was calculated using below formula:

$$\delta = \frac{L}{Z \times A}$$

in which δ [unit: S/cm] is the electrical conductivity of the membrane, Z [unit: Ω] is the electrical impedance, A [unit: cm^2] is the surface area of the electrodes, and L [unit: cm] is the thickness of the membrane or the distance between two electrodes. The thickness of all tested membranes and the diameter of the electrode, therefore, were measured. Solartron provided the electrical impedance of the membranes.

Some small pieces of each membrane were soaked in water overnight for pre-treatment (Figure 41).

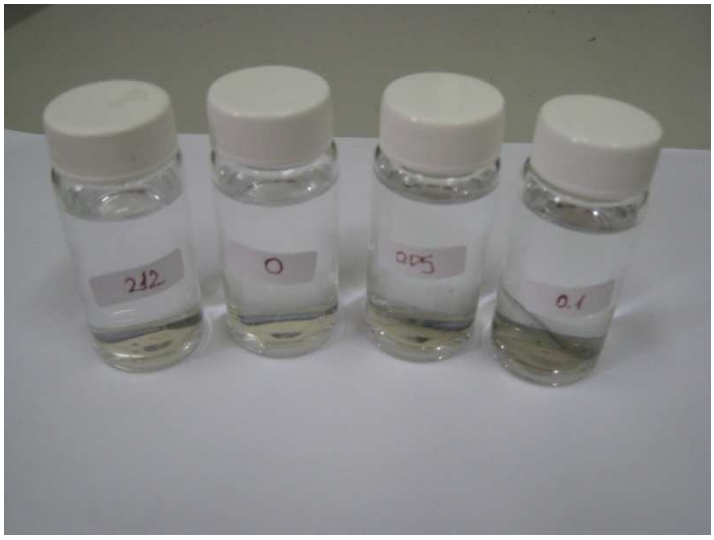

Figure 41. Pre-treatment of membranes for conductivity test.

To start off, Solartron ECI testing module was used to make sure the instrument was in good condition (Figure 42). Plot on Zview generated frequency data and the real and imaginary parts of the impedance so that the values can be compared with those on ECI Test Module tabulated table. The membrane was put in between two identical electrodes (Figure 43) and then inside the Temperature and Humidification Controller THC (Figure 44).

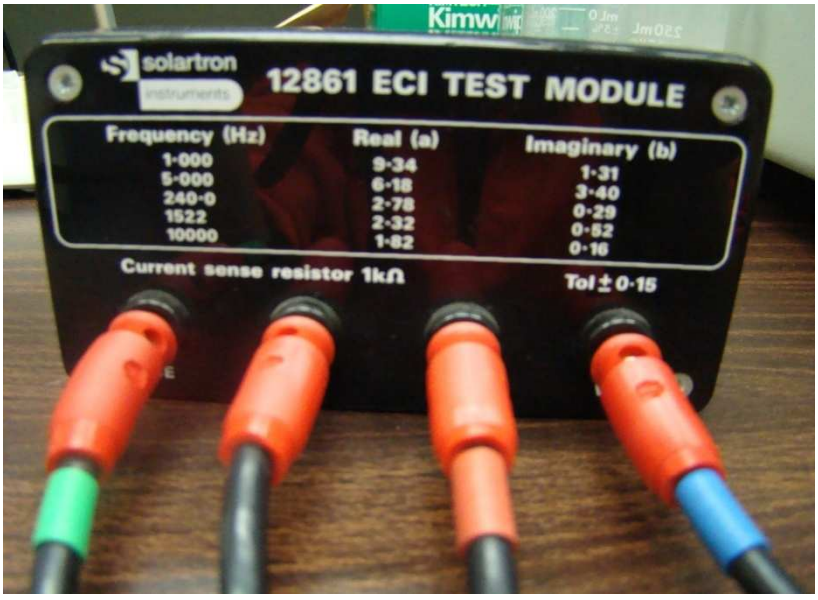

Figure 42. Solartron ECI Test Module.

Figure 43. Membrane in-between two electrodes (on the left) and inside the THC (on the right).

Figure 44. THC manufactured by Giant Force Instrument Enterprise Co., Ltd., Taiwan.

To collect impedance for membranes, “Sweep Frequency” was set at an initial value of 10^6 Hz and final value of 0.1 Hz. At first, the temperature was set at 20°C and the humidification was at 100%. The system was left at 100% humidity and 20°C for about two hours to stabilize and then data were collected using “Measure Sweep” mode. Sequentially, impedance data were collected for the membrane at temperatures of 40°C, 60°C, 80°C, and 95°C. The humidity was maintained at 100% during the whole process. The higher the temperature, the higher the water uptake by the membranes, the shorter time it takes for the membrane to reach approximately 100% humid at a certain temperature. Nevertheless, it was important that the membranes were given enough time to stabilize their conditions for accurate testing. The membranes were, therefore, left inside the THC for more than one hour to two hours each at 20°C and 40°C, for around 40 minutes each at 60°C and 80°C, and for fifteen minutes at 95°C.

Chapter 4. RESULTS AND DISCUSSION

4.1. Successful Modification of PVA onto MWCNTs

4.1.1. Fourier Transform Infrared Spectra

IR Spectrum software was used to generate a plot of transmittance (%) vs. wavenumber (cm^{-1}) for CNT-PVA, which was then compared with that of pure CNT (Figure 45).

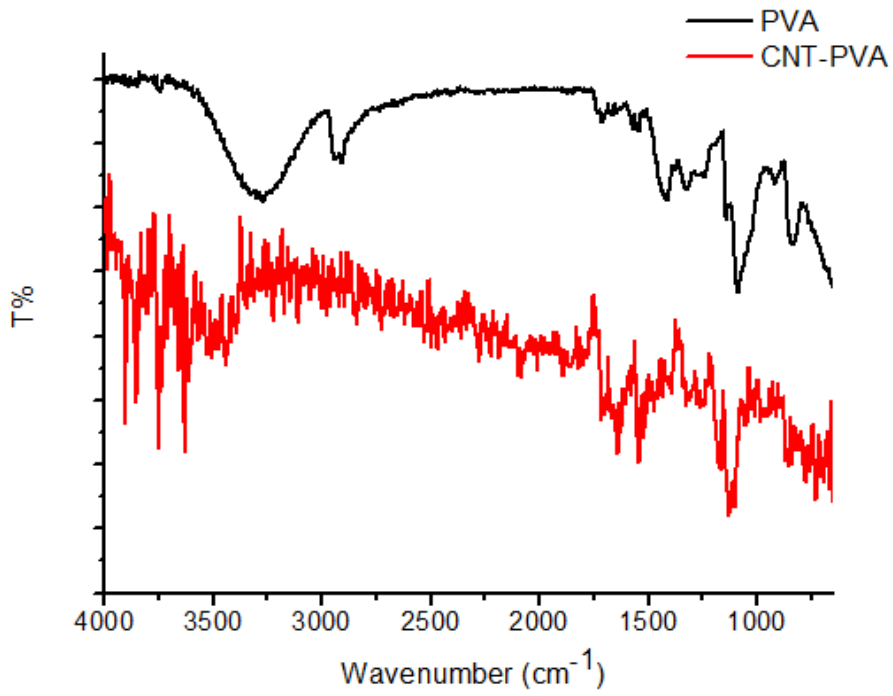

Figure 45. ATR/FTIR spectra of CNT-PVA (red line) and pure PVA (black line).

A broad peak at around 3300 cm^{-1} verified the presence of a hydroxyl group –OH. Strong signal at 1150 cm^{-1} was the proof of C-O bond. These two peaks were clear evidences of the successful attachment of PVA on the MWCNTs surface. Corresponding stretches on PVA plot were hydroxyl group from 3000 – 3600 cm^{-1}, and C-O bonding in the region of 1000 – 1250 cm^{-1}. Also, the peak at around 2850 – 2900 cm^{-1} on IR curve of PVA was an indication of CH/CH_2 bonding. On the other hand, on the IR curve of CNT-PVA, some peaks were seen at around

1550 – 1750 cm^{-1}, which originated from C-C bonding indicating the presence of both CNT and PVA.

4.1.2. Thermogravimetric Analysis Thermogram

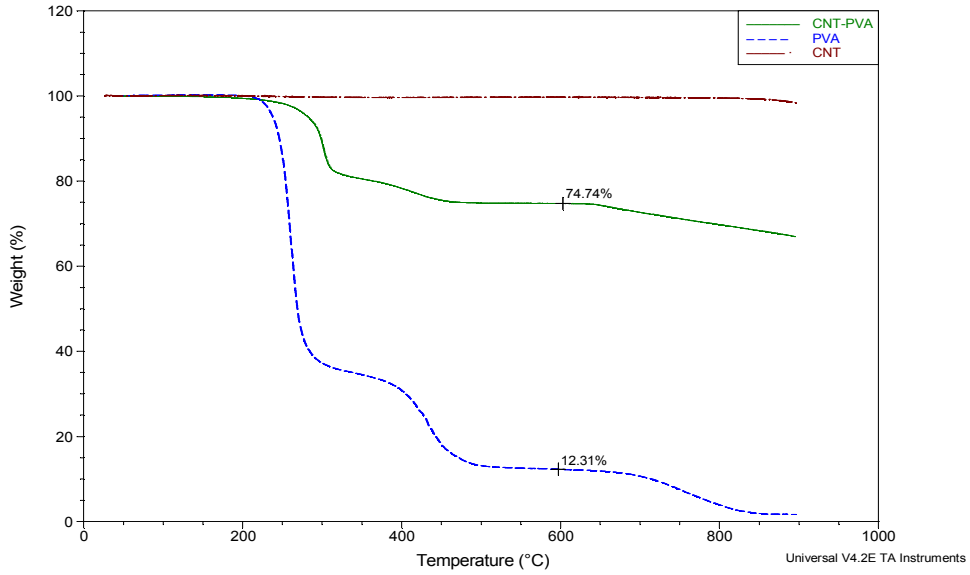

Figure 46. TGA thermogram of CNT-PVA (green), pure MWCNTs (brown), and pure PVA (blue).

Under nitrogen condition, at 600°C, pristine MWCNTs did not demonstrate any significant weight loss while dry PVA exhibited a dramatic weight loss of more than 87%. The weight loss of CNT-PVA hybrid in its TGA thermogram corresponded to the amount of PVA, which was about 25% of total collected sample. Most of the PVA weight loss occurred at 600°C, where PVA was completely degraded, thus this point was considered characteristic temperature of PVA.

4.1.3. X-ray Photoelectron Spectra

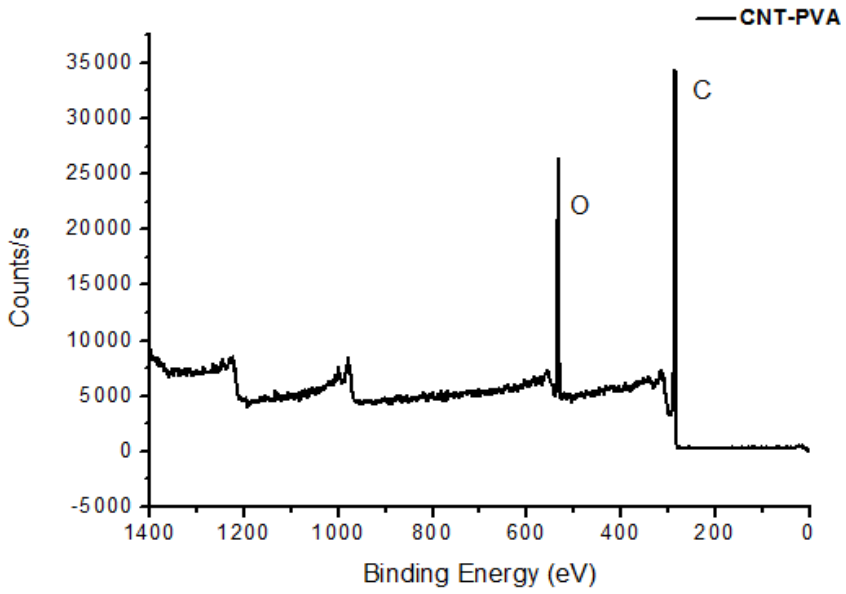

Figure 47. Wide-scan XPS of CNT-PVA.

The large oxide signal on the spectrum in Figure 47 indicated the success of incorporating PVA to CNTs. In Figure 48, besides the major peak at 285 eV, CNT-PVA showed peak components with binding energies at 285.48 eV for O═C-C species, 286.5 eV for C-O species, and 290.13 eV for O═C-O species. These peak assignments corresponded to the chemical structure of PVA synthesized form polyvinyl acetate.

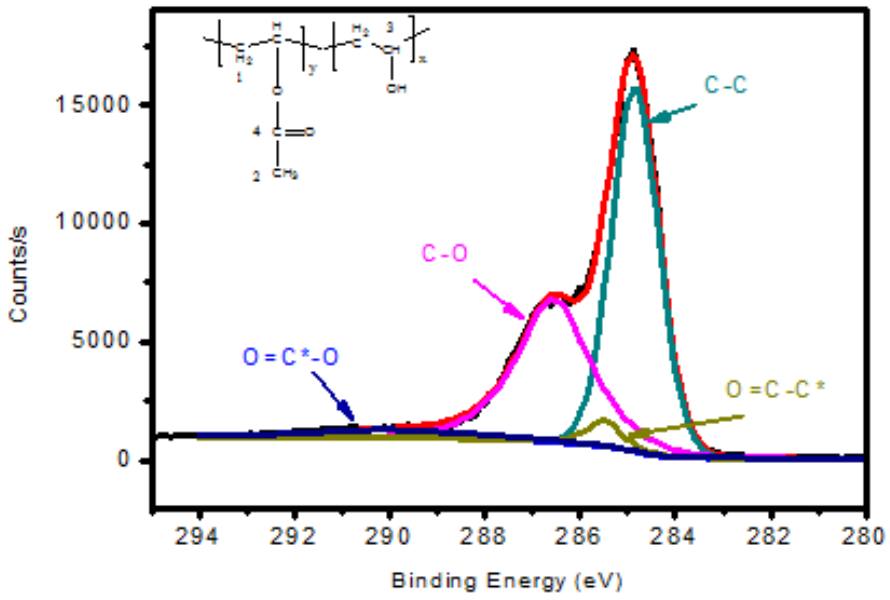

Figure 48. The C 1s core-level spectrum of CNT-PVA.

4.1.4. Solubility Test Observation

As shown in Figure 49, the difference between two samples can be physically tested. On the left, CNTs modified by PVA was relatively easy to be dissolved in water, only tiny particles could be seen floating inside. On the right, however, pristine MWCNTs did not dissolve well in water and completely sank down to the bottom. This observation provided additional evidence of the successful preparation of CNT-PVA.

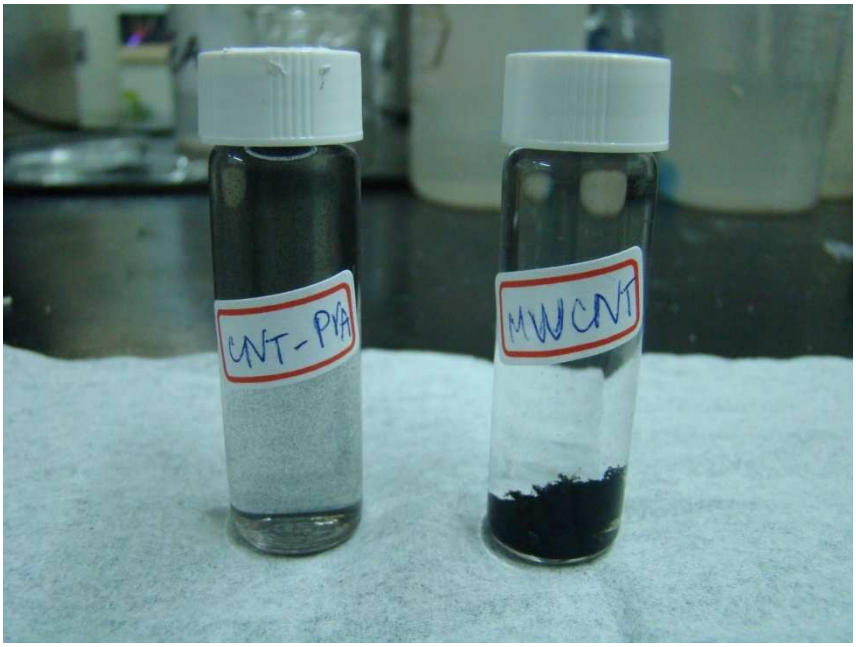

Figure 49. Solubility test results.

4.2. Characterization of CNT-PVA/Nafion Composite Membranes

4.2.1. Mechanical Properties

BlueHill software used for Instron test generated a stress-strain curve for each kind of membrane tested. Both of the composite membranes exhibited better stress than that of commercial Nafion 212 and better strain than that of recast Nafion (Figure 50). Although there was no considerable difference in Young's modulus values among those of composite membranes and those of recast membrane, significant improvements in maximum tensile strength verified high compatibility between CNT-PVA additives and Nafion matrix (Table 4). The increased mechanical strength associated with the fabrication of Nafion membranes with PVA-functionalized-CNTs could potentially reduce the failure of membranes in hydrated states for fuel cell applications. [See Appendix A for Instron test data]

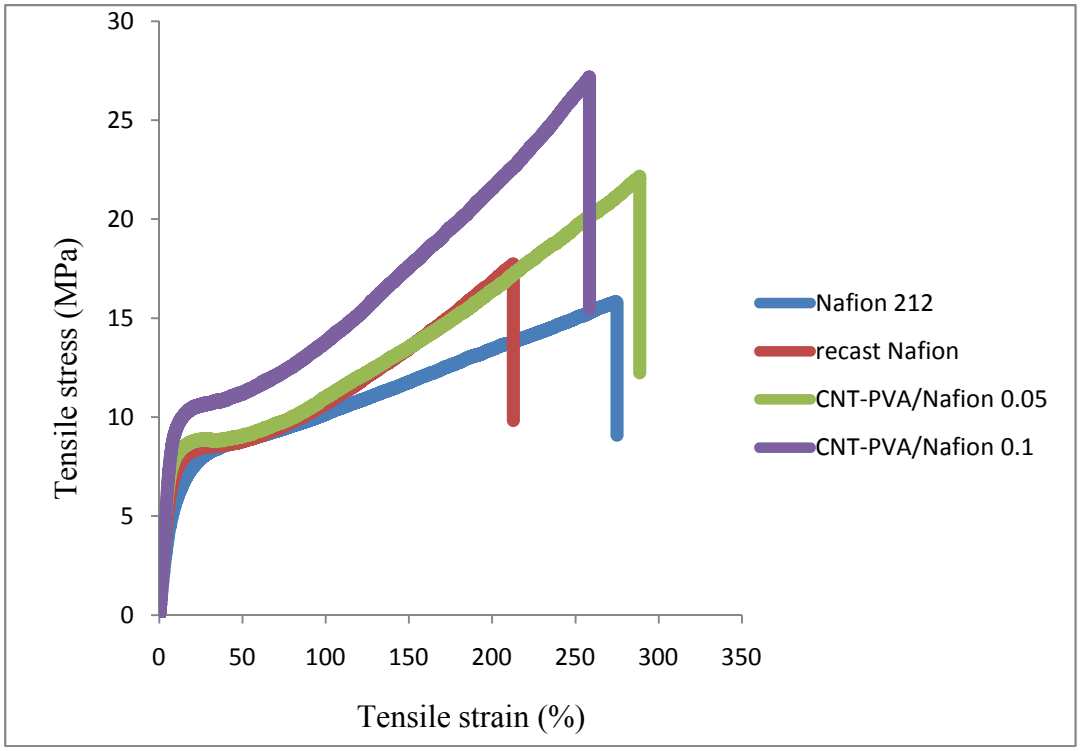

Figure 50. Stress –strain curve of all membranes in comparison.

Table 4. Mechanical strength values extracted from Instron test for commercial Nafion 212, Nafion recast, and two composite membranes.

Membrane	**Nafion 212**	**Recast Nafion**	**CNT-PVA/Nafion 0.05**	**CNT-PVA/Nafion 0.1**
Maximum stress (MPa)	16	18	27	22
Maximum strain (%)	275	212	258	288
Young's modulus (MPa)	61	99	110	114

.

4.2.2. Proton Conductivity

Results found from the proton conductivity test showed that Nafion composite membranes did not have as high performance as that of commercial Nafion. At 95°C, the proton conductivity of Nafion 212 was approximately 0.04 S/cm while that of CNT-PVA/Nafion 0.1 was about 0.035 S/cm and that of CNT-PVA/Nafion 0.05 was only 0.021 S/cm (Figure 51). However, the gap between the proton conductivity values of CNT-PVA/Nafion 0.1 and those of Nafion 212 was not as wide as that between corresponding values CNT-PVA/Nafion 0.05 and Nafion 212; therefore, increasing the content of incorporated CNT-PVA might be considered a reasonable option for future research. [See Appendix B for proton conductivity test data]

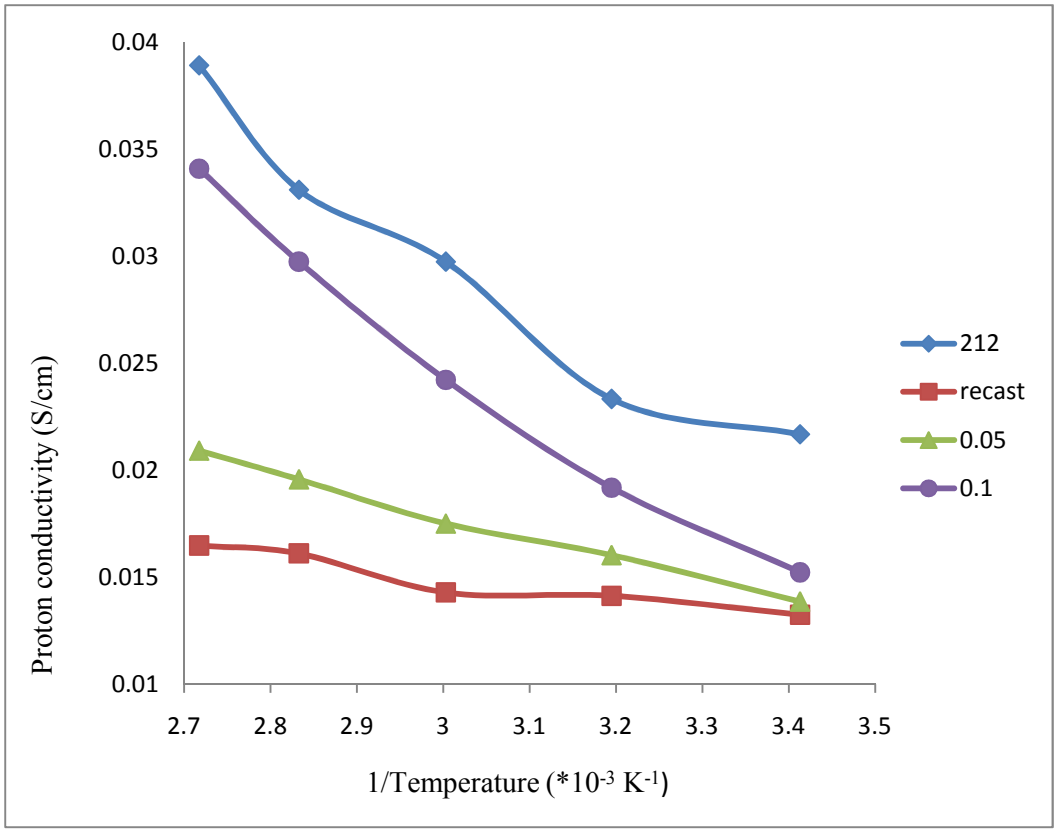

Figure 51. Temperature-dependent proton conductivity of Nafion 212, recast Nafion, CNT-PVA/Nafion 0.05, and CNT-PVA/Nafion 0.1.

Chapter 5. CONCLUSIONS

- Ozone-mediated method was exploited to successfully incorporate PVA to MWCNTs, proving its potential for use in functionalization of CNTs with other high performing polymers.
- ATR-FTIR spectroscopy, TGA analysis, XPS spectrometry, and solubility test were persuasive for the confirmation of the attachment of PVA on CNT surfaces.
- Instron test verified the hypothesis that CNT-PVA/Nafion composite membranes possess better mechanical properties than Nafion 212 and recast Nafion membranes.
- Proton conductivity test showed that commercial Nafion 212 membranes still possess higher conductivities than those of composite CNT-PVA/Nafion membranes.

Chapter 6. RECOMMENDATIONS FOR FUTURE WORK

- Other instrumental tools such as Raman spectra or high resolution transmission electron microscope (HRTEM) might also be used to affirm the formation of CNT-PVA.
- Further investigation will be needed to figure out how to maintain improved mechanical strength of the composite membranes without dropping their proton conductivity in comparison with commercial Nafion membranes.
- Suggestions for promising change in conductivity values as well as cell performance include increasing the content of CNT-PVA in nanocomposite membranes, or using other polymers for better dispersion or interaction within Nafion matrix.

REFERENCES

"An exploded view of PEMFC components." *Energi DTU Kemi*. Web. 9 Dec 2010. <http://www.energi.kemi.dtu.dk/Projekter/fuelcells.aspx>.

"Collecting the History of Proton Exchange Membrane Fuel Cells." *American History*. Smithsonian Institution, 2004. Web. 9 Dec 2010. <http://americanhistory.si.edu/fuelcells/pem/pemmain.htm>.

Hickner Michael A., Ghassemi Hossein, Kim Yu Seung, Einsla Brian R., McGrath James E. "Alternative Polymer Systems for Proton Exchange Membranes (PEMs)." *American Chemical Society*. 104. (2004): 4587-4612.

Hoogers, G. *Fuel Cell Technology Handbook*. CRC Press LLC, 2003.

Liu, Ying-Ling, and Chia-Ming Chang. "Functionalization of multi-walled carbon nanotubes with non-reactive polymers through an ozone-mediated process for the preparation of a wide range of high performance polymer/carbon nanotube composites." *ScienceDirect*. 48. (2009): 1289-1297.

Liu, Ying-Ling, Chia-Ming Chang, Yu-Huei Su, Da-Ming Wang, and Juin-Yih Lai. "Preparation and applications of Nafion-functionalized multiwalled carbon nanotubes for proton exchange membrane fuel cells." *Journal of Materials Chemistry*. 20. (2010): 4409-4416.

Liu, Ying-Ling, Yu-Hsun Chang, and Mong Liang. "Poly(2,6-dimethyl-1,4-phenylene oxide) (PPO) multi-bonded carbon nanotube (CNT): Preparation and formation of PPO/CNT nanocomposites." *Polymer*. 49. (2008): 5405-5409.

Liu, Yong-Hao, Baolian Yi, Zhi-Gang Shao, Danmin Xing, and Huamin Zhang. "Carbon Nanotubes Reinforced Nafion Composite Membrane for Fuel Cell Applications." *Electrochemical and Solid-State Letters*. 9. (2006): A356-A359.

Pillai, Vijayamohanan K., Ramaiyan Kannan, and Bhalchandra A. Kakade. "Polymer Electrolyte Fuel Cells Using Nafion-Based Composite Membranes with Functionalized Carbon Nanotubes." *Angewandte Chemie*. 47. (2008): 2653-2656.

Pillai, Vijayamohanan K., Ramaiyan Kannan, Meera Parthasarathy, Sreekuttan U. Maraveedu, and Sreekumar Kurungot. "Domain Size Manipulation of Perflouorinated Polymer Electrolytes by Sulfonic Acid-Functionalized MWCNTs To Enhance Fuel Cell Performance." *Langmuir*. 25. (2009): 8299-8305.

Pillai, Vijayamohanan K., Ramaiyan Kannan, Pradnya P. Aher, Thangavelu Palaniselvam, and Sreekumar Kurungot. "Artificially Designed Membranes Using Phosphonated-Multiwall Carbon Nanotube-Polybenzimidazole Composites for Polymer Electrolyte Fuel Cells ." *Journal of Physical Chemistry Letters*. 9. (2010): 4.61.

"Polyvinyl Alcohol MSDS." *ScienceLab*. Web. 9 Dec 2010. <http://www.sciencelab.com/msds.php?msdsId=9927396>.

"Schematic of Proton Exchange Membrane Fuel Cell ." *Fuel Cells Working Concept*. Web. 9 Dec 2010. <http://www.hydrogen-fc.com/fuel-cells-working-concept/>.

Skoog, Douglas A., F. James Holler, and Timothy A. Nieman. *Principle of Instrumental Analysis*. 5th Ed. Brooks Cole.

Thomassin, Jean-Michel, Jozef Kollar, Giuseppe Caldarella, Albert Germain, and Christophe Detrembleur. "Beneficial effect of carbon nanotubes on the performances of Nafion membranes in fuel cell applications." *Journal of Membrane Science*. 303. (2007): 252-257.

APPENDICES

Appendix A. Instron data for each membrane taken to calculate Young's modulus

Table 5. Instron test data taken for recast Nafion membrane.

0	**-0.00937**	**1.597612**	**1.947134**	**3.195224**	**3.749604**	**4.792836**	**5.147522**
0.003658	0.004626	1.640771	2.026832	3.239115	3.82688	4.839653	5.194631
0.059984	0.087473	1.677346	2.065146	3.276421	3.88013	4.877691	5.226593
0.108995	0.16435	1.71319	2.106262	3.313728	3.883899	4.914998	5.294172
0.152885	0.154487	1.757081	2.157686	3.35835	3.935568	4.954499	5.283244
0.19897	0.218917	1.798777	2.17946	3.394926	3.945133	4.993269	5.291053
0.233351	0.276583	1.8295	2.218243	3.427844	3.985579	5.028382	5.292102
0.269195	0.34225	1.866075	2.273051	3.468076	4.035837	5.07154	5.341687
0.313085	0.407806	1.912892	2.339251	3.517819	4.082872	5.116894	5.351611
0.351124	0.415847	1.952393	2.369102	3.5522	4.119512	5.147617	5.396254
0.38843	0.503746	1.9897	2.407272	3.585118	4.141064	5.183461	5.391784
0.431589	0.516742	2.029933	2.457722	3.626814	4.224008	5.228083	5.479624
0.468165	0.563995	2.066508	2.501303	3.667778	4.235949	5.266853	5.439748
0.501814	0.620709	2.100889	2.539346	3.703622	4.257937	5.303429	5.521399
0.542047	0.651067	2.14478	2.586204	3.746049	4.331099	5.343661	5.566545
0.591058	0.670375	2.191596	2.667922	3.785551	4.317232	5.384626	5.560671
0.62617	0.742193	2.221588	2.759922	3.819932	4.345783	5.419738	5.590771
0.65982	0.824849	2.257432	2.742695	3.85797	4.392641	5.460703	5.609131
0.700784	0.841275	2.301322	2.781582	3.904787	4.447955	5.506056	5.634486
0.739554	0.927925	2.341555	2.830718	3.942093	4.438591	5.537511	5.670817
0.777592	0.92888	2.378862	2.922433	3.973548	4.485874	5.571892	5.649734
0.821483	1.025098	2.418363	2.957207	4.015976	4.538984	5.617977	5.681656
0.860984	1.068304	2.459328	2.949574	4.059135	4.552308	5.661867	5.709741
0.893902	1.110441	2.493709	3.007284	4.09571	4.635792	5.696979	5.710793
0.93194	1.12848	2.533941	3.053009	4.135211	4.683212	5.733555	5.805223
0.979488	1.198709	2.58149	3.056544	4.176176	4.691394	5.774519	5.82107
1.015332	1.245369	2.612944	3.120696	4.210557	4.727658	5.809631	5.830494
1.04825	1.280069	2.646594	3.166499	4.247132	4.730164	5.849133	5.814553
1.089215	1.326796	2.691947	3.234363	4.295411	4.760414	5.897412	5.831587
1.133836	1.373144	2.734375	3.25806	4.334913	4.818013	5.93033	5.877453
1.170412	1.468039	2.769487	3.30204	4.366368	4.814636	5.96398	5.897209
1.211376	1.478439	2.806062	3.344904	4.405138	4.831672	6.006407	5.928924
1.250878	1.500564	2.847758	3.445695	4.449028	4.942716	6.050298	5.935229
1.284527	1.569062	2.884333	3.472079	4.485603	4.943027	6.084678	6.009751
1.320371	1.609152	2.923103	3.467704	4.525105	4.974785		
1.369382	1.675325	2.971383	3.537555	4.567532	4.980069		
1.408883	1.697474	3.004301	3.55036	4.602644	5.03561		
1.440338	1.751618	3.03795	3.598122	4.637756	5.007149		
1.479108	1.848212	3.080377	3.643043	4.682378	5.091826		
1.522998	1.873788	3.125731	3.669079	4.724074	5.09723		
1.559574	1.919658	3.160112	3.734414	4.755529	5.14196		

Table 6. Instron data taken for Nafion 212.

0	-0.00526	2.260593	1.929346	4.515889	3.552875	6.780719	4.678372
0.004237	-0.02097	2.32733	1.99901	4.582626	3.602701	6.834744	4.697758
0.048729	0.006893	2.370762	2.041221	4.637711	3.604507	6.897245	4.720821
0.148305	0.180073	2.423729	2.059158	4.684321	3.649008	6.95021	4.741409
0.21928	0.169197	2.488347	2.162241	4.740465	3.672061	6.999999	4.753527
0.275424	0.123005	2.542373	2.154928	4.808262	3.704535	7.06038	4.788222
0.341102	0.266739	2.596398	2.220497	4.863347	3.745626	7.129236	4.82221
0.401483	0.364151	2.658898	2.297808	4.912075	3.76291	7.172668	4.825434
0.447034	0.354819	2.715042	2.303347	4.971398	3.794553	7.224575	4.867264
0.503178	0.353682	2.76483	2.355428	5.028601	3.821899	7.291312	4.889003
0.573093	0.43012	2.823093	2.392082	5.082626	3.860799	7.350634	4.90157
0.623941	0.524219	2.88983	2.448499	5.147245	3.900306	7.401482	4.925755
0.673729	0.583692	2.93644	2.506483	5.204448	3.935978	7.457625	4.93274
0.733051	0.564015	2.988347	2.528451	5.249999	3.963535	7.516948	4.966199
0.792373	0.616272	3.054025	2.579682	5.301906	3.974592	7.565676	4.966844
0.846398	0.70982	3.112288	2.60767	5.371821	4.031467	7.623939	4.998788
0.908898	0.792311	3.164194	2.66356	5.432203	4.071159	7.695973	5.03496
0.967161	0.793139	3.221398	2.731061	5.478813	4.077413	7.743643	5.041678
1.013771	0.839685	3.28072	2.759604	5.537075	4.12257	7.791312	5.0537
1.065678	0.879114	3.328389	2.762616	5.596397	4.143891	7.851693	5.070579
1.137712	0.976457	3.386652	2.823024	5.648304	4.156983	7.913135	5.092406
1.193856	1.009079	3.457627	2.886822	5.705508	4.195306	7.963982	5.130515
1.240466	1.016373	3.505296	2.904535	5.768008	4.212765	8.021185	5.134965
1.297669	1.069857	3.554025	2.930443	5.818855	4.228949	8.082626	5.154808
1.356991	1.177549	3.615465	3.001652	5.870762	4.270421	8.134533	5.187428
1.409957	1.210545	3.675847	3.034581	5.93644	4.31085	8.189617	5.188795
1.469279	1.240964	3.727754	3.057893	5.995762	4.337205	8.254236	5.225391
1.53072	1.294457	3.781779	3.106847	6.041313	4.347695		
1.580508	1.371949	3.845338	3.149996	6.096398	4.384329		
1.632415	1.388977	3.897245	3.142023	6.162076	4.396993		
1.699152	1.429062	3.95233	3.188368	6.216101	4.444927		
1.758474	1.510065	4.020127	3.249669	6.271186	4.463435		
1.804025	1.565315	4.070974	3.250668	6.330508	4.488705		
1.85911	1.58624	4.117584	3.300219	6.383474	4.518191		
1.924788	1.64698	4.176906	3.325509	6.433262	4.51612		
1.978813	1.717237	4.244703	3.36776	6.49894	4.559224		
2.036017	1.789551	4.296609	3.403461	6.564618	4.60273		
2.095339	1.786698	4.349576	3.441683	6.609109	4.605985		
2.146186	1.839327	4.407838	3.459878	6.661016	4.634197		
2.195974	1.887646	4.461864	3.5203	6.725634	4.651827		

Table 7. Instron data taken for CNT-PVA/Nafion 0.05 membrane.

0	0.019394	1.536578	2.250764	3.069556	4.33209	4.608294	5.881251
0.00216	-0.01126	1.579061	2.317588	3.115639	4.398493	4.647176	5.913811
0.021601	0.042366	1.612903	2.391857	3.151641	4.409039	4.688939	5.947556
0.098646	0.195654	1.648185	2.431381	3.183323	4.453312	4.723501	5.985273
0.15049	0.248407	1.690668	2.473659	3.222206	4.49703	4.757344	5.972903
0.187932	0.221287	1.72739	2.57712	3.267569	4.536297	4.799106	6.045593
0.234015	0.324907	1.766993	2.622417	3.305731	4.576533	4.847349	6.091289
0.272177	0.421517	1.809476	2.67257	3.341733	4.652328	4.879032	6.082802
0.304579	0.453733	1.844038	2.717816	3.381336	4.685759	4.912154	6.112787
0.343462	0.464772	1.87716	2.758668	3.417338	4.748223	4.954636	6.165448
0.388105	0.51534	1.918202	2.80776	3.45262	4.760597	4.993519	6.179593
0.424827	0.606503	1.966446	2.887911	3.497983	4.818684	5.029521	6.229345
0.46155	0.718076	1.998128	2.921278	3.539026	4.862211	5.072724	6.242522
0.501872	0.705569	2.03269	2.964469	3.569988	4.923606	5.109446	6.27954
0.537154	0.756658	2.074453	3.049687	3.60671	4.935123	5.143288	6.302657
0.571717	0.813404	2.112615	3.125128	3.650633	5.005583	5.182891	6.31278
0.616359	0.922572	2.150057	3.15006	3.688796	5.023598	5.229694	6.357501
0.659562	0.959376	2.19398	3.189613	3.724798	5.113574	5.262096	6.403504
0.690524	0.991346	2.229982	3.247438	3.7644	5.129993	5.295218	6.405708
0.726526	1.028097	2.263104	3.301043	3.803283	5.153878	5.339141	6.420781
0.769009	1.134	2.301987	3.34855	3.837845	5.210711	5.378023	6.483152
0.807892	1.185224	2.34807	3.400533	3.880328	5.209057	5.415466	6.50674
0.843894	1.183205	2.381192	3.45713	3.922811	5.277021	5.455068	6.501001
0.885657	1.27436	2.415034	3.479176	3.953773	5.299149	5.493951	6.542372
0.922379	1.346798	2.459677	3.57381	3.989055	5.312576	5.527073	6.547767
0.957661	1.390685	2.49928	3.610082	4.036578	5.336667	5.564515	6.562133
0.999424	1.444388	2.535282	3.706053	4.07546	5.391764	5.613478	6.632598
1.043347	1.491201	2.576324	3.726267	4.108582	5.436913	5.649481	6.610394
1.073589	1.57108	2.614487	3.755917	4.147465	5.454505	5.681883	6.656339
1.108871	1.637486	2.646889	3.818499	4.187067	5.509341	5.722205	6.673228
1.155674	1.698137	2.685051	3.83675	4.22163	5.543737		
1.194556	1.732906	2.734015	3.915028	4.261952	5.59508		
1.229118	1.806209	2.768577	3.942698	4.306595	5.604515		
1.266561	1.860084	2.800259	3.990004	4.340437	5.675974		
1.306883	1.921511	2.840581	4.047919	4.374999	5.66334		
1.342166	1.968464	2.882344	4.094939	4.416762	5.722473		
1.381768	2.020106	2.918346	4.177196	4.459245	5.760433		
1.426411	2.091414	2.957229	4.213947	4.492367	5.765556		
1.459533	2.145705	2.997551	4.212015	4.529089	5.809278		
1.493375	2.172338	3.033554	4.334135	4.572292	5.838909		

Table 8. Instron data taken for CNT-PVA/Nafion 0.1 membrane.

0	0.010653	2.073317	2.569124	4.13888	5.558164	6.200565	7.683389
0.005816	0.040147	2.120812	2.635934	4.19316	5.624801	6.260661	7.747
0.08239	0.066469	2.166369	2.632055	4.23387	5.676361	6.310095	7.765586
0.154118	0.12905	2.224527	2.787446	4.283304	5.708705	6.354683	7.811034
0.201613	0.156439	2.273961	2.940202	4.347277	5.838668	6.405086	7.856508
0.26074	0.217686	2.324364	2.922846	4.39865	5.894648	6.469059	7.862883
0.317928	0.155694	2.38446	3.00095	4.446146	5.940404	6.516554	7.928051
0.357669	0.280149	2.431955	3.08552	4.497518	5.990843	6.561142	7.944395
0.406134	0.273901	2.476543	3.160511	4.54986	6.064691	6.615422	8.031852
0.471076	0.334459	2.527915	3.268018	4.596386	6.083422	6.670672	8.050991
0.522449	0.377434	2.590919	3.321053	4.651636	6.154624	6.718167	8.080811
0.568975	0.378264	2.641322	3.39462	4.71367	6.267563	6.774386	8.140983
0.620347	0.575069	2.684941	3.489463	4.756319	6.299212	6.827697	8.149232
0.672689	0.529676	2.739221	3.60335	4.802845	6.350145	6.873254	8.239293
0.718246	0.608806	2.792532	3.641633	4.860033	6.467422	6.922688	8.195592
0.775434	0.650932	2.840028	3.732356	4.912375	6.494883	6.982784	8.252887
0.8365	0.750848	2.896247	3.841165	4.961809	6.589903	7.033188	8.276482
0.878179	0.822477	2.950527	3.900293	5.013182	6.625278	7.076806	8.327234
0.923736	0.843799	2.996084	3.979695	5.069401	6.614569	7.131086	8.326549
0.981894	0.928532	3.045517	4.012002	5.115927	6.766766	7.189243	8.363271
1.036174	1.010389	3.104644	4.082815	5.168269	6.734414	7.236739	8.474953
1.084638	1.14396	3.156017	4.151744	5.228365	6.829692	7.28908	8.486973
1.136011	1.137925	3.199635	4.217366	5.271014	6.888707	7.342392	8.543215
1.191261	1.227645	3.254885	4.357389	5.31657	6.886942	7.388918	8.525664
1.237787	1.348683	3.312073	4.417819	5.374728	6.987194	7.438352	8.538614
1.290129	1.36029	3.360538	4.52877	5.433855	6.982856	7.500386	8.572518
1.353133	1.440981	3.414818	4.559753	5.48135	7.07446	7.555636	8.553384
1.394812	1.557377	3.46619	4.63748	5.528846	7.086765	7.596347	8.587116
1.440369	1.568158	3.511747	4.742201	5.584095	7.212177	7.64675	8.608637
1.499496	1.670488	3.561181	4.784168	5.63256	7.312098	7.705877	8.669358
1.557653	1.729349	3.623216	4.831314	5.682963	7.230386		
1.604179	1.83417	3.677496	4.918856	5.746936	7.322779		
1.651675	1.906194	3.719176	5.028936	5.791524	7.335416		
1.706924	2.041184	3.76861	5.054137	5.836111	7.407313		
1.75442	2.058418	3.828706	5.139438	5.889422	7.427037		
1.805792	2.122805	3.876201	5.200136	5.950488	7.520451		
1.870735	2.24829	3.928543	5.317621	5.997983	7.522761		
1.914353	2.312069	3.983793	5.395544	6.04354	7.555975		
1.95991	2.341754	4.032257	5.429893	6.101697	7.616755		
2.013221	2.470742	4.079753	5.459482	6.151131	7.696475		

Appendix B. Proton conductivity data taken for Nafion 212, recast Nafion, CNT-PVA/Nafion 0.05 and CNT-PVA/Nafion 0.1.

Table 9. Proton conductivity test data for all membranes at interval temperature at relative humidity 100%.

Membrane	T(°C)	d (cm)	A (cm^2)	R (Ω)	□ (S/cm)	1/T (*10^{-3} K^{-1})
Nafion 212	20	0.007	1.32665	0.2433	0.021687	3.412969
	40	0.007	1.32665	0.2261	0.023337	3.194888
	60	0.007	1.32665	0.1774	0.029743	3.003003
	80	0.007	1.32665	0.1594	0.033102	2.832861
	95	0.007	1.32665	0.1356	0.038912	2.717391
Nafion recast	20	0.0062	1.32665	0.3526	0.013254	3.412969
	40	0.0062	1.32665	0.3306	0.014136	3.194888
	60	0.0062	1.32665	0.3269	0.014296	3.003003
	80	0.0062	1.32665	0.29	0.016115	2.832861
	95	0.0062	1.32665	0.2835	0.016485	2.717391
CNT-PVA/Nafion 0.05	20	0.0035	1	0.2525	0.013861	3.412969
	40	0.0035	1	0.2183	0.016033	3.194888
	60	0.0035	1	0.1999	0.017509	3.003003
	80	0.0035	1	0.17878	0.019577	2.832861
	95	0.0035	1	0.1673	0.020921	2.717391
CNT-PVA/Nafion 0.1	20	0.0041	1	0.26917	0.015232	3.412969
	40	0.0041	1	0.21372	0.019184	3.194888
	60	0.0041	1	0.16924	0.024226	3.003003
	80	0.0041	1	0.13785	0.029742	2.832861
	95	0.0041	1	0.12027	0.03409	2.717391